NAVAL POSTGRADUATE SCHOOL

MONTEREY, CALIFORNIA

THESIS

VIBRATIONAL ANALYSIS OF A SHIPBOARD FREE ELECTRON LASER BEAM PATH

by

Bryan M. Gallant

December 2011

Thesis Advisor:	William Colson
Second Reader:	Keith Cohn

Approved for public release; distribution is unlimited

THIS PAGE INTENTIONALLY LEFT BLANK

REPORT DOCUMENTATION PAGE			Form Approved OMB No. 0704-0188
Public reporting burden for this collection of information is estimated to average 1 hour per response, including the time for reviewing instruction, searching existing data sources, gathering and maintaining the data needed, and completing and reviewing the collection of information. Send comments regarding this burden estimate or any other aspect of this collection of information, including suggestions for reducing this burden, to Washington headquarters Services, Directorate for Information Operations and Reports, 1215 Jefferson Davis Highway, Suite 1204, Arlington, VA 22202-4302, and to the Office of Management and Budget, Paperwork Reduction Project (0704-0188) Washington DC 20503.			
1. AGENCY USE ONLY ***(Leave blank)***	**2. REPORT DATE** December 2011	**3. REPORT TYPE AND DATES COVERED** Master's Thesis	
4. TITLE AND SUBTITLE Vibrational Analysis of a Shipboard Free Electron Laser Beam Path		**5. FUNDING NUMBERS**	
6. AUTHOR(S) Bryan M. Gallant			
7. PERFORMING ORGANIZATION NAME(S) AND ADDRESS(ES) Naval Postgraduate School Monterey, CA 93943-5000		**8. PERFORMING ORGANIZATION REPORT NUMBER**	
9. SPONSORING /MONITORING AGENCY NAME(S) AND ADDRESS(ES) N/A		**10. SPONSORING/MONITORING AGENCY REPORT NUMBER**	
11. SUPPLEMENTARY NOTES The views expressed in this thesis are those of the author and do not reflect the official policy or position of the Department of Defense or the U.S. Government. IRB Protocol Number: N/A			
12a. DISTRIBUTION / AVAILABILITY STATEMENT Approved for public release; distribution is unlimited		**12b. DISTRIBUTION CODE** A	

13. ABSTRACT (maximum 200 words)

This thesis explores the deployment of a free electron laser (FEL) weapon system in a shipboard vibration environment. A concept solid model of a shipboard FEL is developed and used as a basis for a finite element model which is subjected to vibration simulation in MATLAB. Vibration input is obtained from ship shock trials data and wave excited motion data from ship motion simulation software. Emphasis is placed on the motion of electron beam path components of the FEL and the feasibility of operation aboard ship. The resulting component motion after passive isolation control is within the amplitudes and frequencies that will allow at sea FEL operation with active electron beam steering.

14. SUBJECT TERMS Free Electron Laser, FEL, Passive Vibration Control, Ship Motion Simulation, Finite Element Modeling, Directed Energy			**15. NUMBER OF PAGES** 73
			16. PRICE CODE
17. SECURITY CLASSIFICATION OF REPORT Unclassified	**18. SECURITY CLASSIFICATION OF THIS PAGE** Unclassified	**19. SECURITY CLASSIFICATION OF ABSTRACT** Unclassified	**20. LIMITATION OF ABSTRACT** UU

NSN 7540-01-280-5500

Standard Form 298 (Rev. 2-89)
Prescribed by ANSI Std. 239-18

THIS PAGE INTENTIONALLY LEFT BLANK

Approved for public release; distribution is unlimited

VIBRATIONAL ANALYSIS OF A SHIPBOARD FREE ELECTRON LASER BEAM PATH

Bryan M. Gallant
Lieutenant, United States Navy
B.S., North Carolina State University, 2005

Submitted in partial fulfillment of the
requirements for the degree of

MASTER OF SCIENCE IN PHYSICS

from the

NAVAL POSTGRADUATE SCHOOL
December 2011

Author: Bryan M. Gallant

Approved by: William Colson, PhD
Thesis Advisor

Keith Cohn, PhD
Second Reader

Andres Larraza, PhD
Chair, Department of Physics

THIS PAGE INTENTIONALLY LEFT BLANK

ABSTRACT

This thesis explores the deployment of a free electron laser (FEL) weapon system in a shipboard vibration environment. A concept solid model of a shipboard FEL is developed and used as a basis for a finite element model which is subjected to vibration simulation in MATLAB. Vibration input is obtained from ship shock trials data and wave excited motion data from ship motion simulation software. Emphasis is placed on the motion of electron beam path components of the FEL and the feasibility of operation aboard ship. The resulting component motion after passive isolation control is within the amplitudes and frequencies that will allow at sea FEL operation with active electron beam steering.

THIS PAGE INTENTIONALLY LEFT BLANK

TABLE OF CONTENTS

THIS PAGE INTENTIONALLY LEFT BLANK

LIST OF FIGURES

THIS PAGE INTENTIONALLY LEFT BLANK

LIST OF TABLES

THIS PAGE INTENTIONALLY LEFT BLANK

LIST OF ACRONYMS AND ABBREVIATIONS

ASCM	Anti-ship Cruise Missile
CAD-	Computer Aided Design
CIWS	Close-in weapon system
DOF-	Degree of freedom
FEL	Free-electron Laser
FEA	Finite element analysis
FEM	Finite element method
IOT	Inductive output tube
LINAC	Linear accelerator
MDOF	Multiple degree of freedom
RF	Radio frequency
WMO	World Meteorological Organization

THIS PAGE INTENTIONALLY LEFT BLANK

ACKNOWLEDGMENTS

I would like to thank Mike Hatch for contributing a great deal of his time and expertise to this project. His methodology for simulation and readiness to assist each time I broke it was invaluable. Thanks also to Professor Papoulias for his assistance with ship motion simulation and parsing that mountain of data. Thanks to Professor Cohn for providing a key observation at the end of the project. Finally, thanks to Professor Colson for being a tough editor and forcing me to “think physicist”, albeit briefly.

THIS PAGE INTENTIONALLY LEFT BLANK

I. INTRODUCTION

A. BACKGROUND

Anti-Ship Cruise Missiles (ASCM) are a primary threat to modern surface combatants. Large quantities of sub-Mach sea-skimming missiles populate the arsenals of potential adversary states and even some non-state actors. In addition, several states either produce or possess advanced supersonic anti-ship cruise missiles. A robust defense capable of dealing with mass waves of low capability ASCMs intermixed with high velocity threats is required to prevent enemy denial of access to critical areas of operation.

Currently, ASCM defense relies on an overlapping system of interceptor missiles, close-in weapons systems, and decoy countermeasures. Each layer of a modern surface combatant's defense is limited by magazine depth when engaged repeatedly or by multiple threats simultaneously. Critically, interceptor missiles typically are required to share magazine space with strike missiles and anti-submarine rockets. Engagement of supersonic ASCMs is complicated by the drastically reduced timeline for interception, where the time from detection to impact precludes a depth of fire greater than one, even with modern high speed interceptor missiles. The delay in engagement that develops from the fly-out time of interceptor missiles potentially exposes the defended asset to residual impact from high velocity debris even if the intercept is successful.

Equipping surface combatants with Free-Electron Lasers (FELs) for shipboard defense addresses both the need for a deep magazine and rapid engagement of high velocity threats. A ship-borne FEL's "magazine" would only be limited by the fuel source of the ship's electric plant which is routinely replenished at sea. Using light as the medium for energy transfer to the threat ASCM allows essentially instantaneous interception of high velocity threats and defeats threat missile evasive maneuvering.

B. PRINCIPLES OF FREE-ELECTRON LASER OPERATION

All lasers use optical amplification to generate coherent light as a medium for energy transfer. Free-electron lasers generate the light used for amplification by passing a

high-energy relativistic electron beam through an alternating transverse magnetic field generated by an undulator consisting of alternating opposed pairs of permanent magnets.

The relativistic electron beam is generated by injecting electrons from a cathode into a Linear Accelerator (LINAC) driven by a Radio Frequency (RF) energy source, such as an Inductive Output Tube (IOT).

Photons are released due to synchrotron radiation as the electron beam takes a sinusoidal path through the undulator. The emitted photons are reflected between two mirrors to build a coherent beam over many passes. One mirror is semitransparent allowing a certain percentage of the photons to be emitted as a coherent laser.

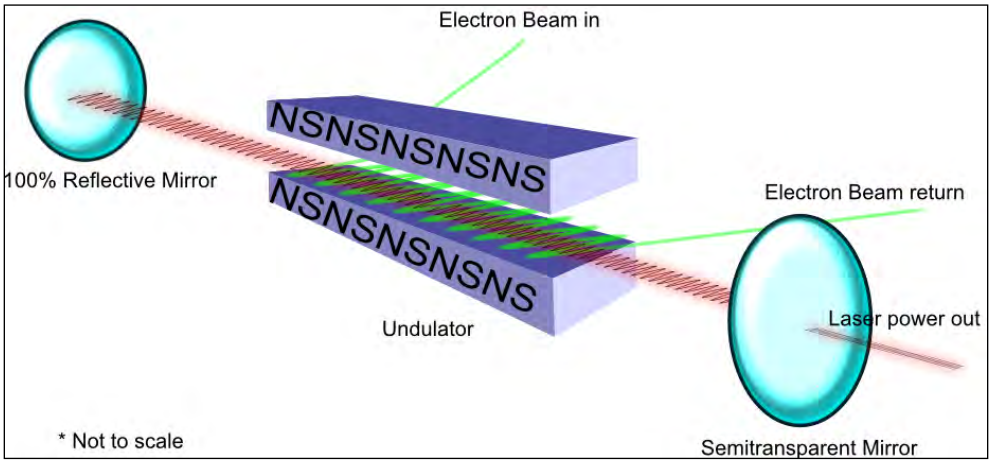

Figure 1. FEL Operation

C. FEL MAJOR COMPONENTS

1. Electron Beam Path

The injector is the source which supplies the electron beam to the LINAC. In the photo-injector design, electrons in the injector's cathode material are ejected after absorbing energy from photons applied by a laser pulsed at several hundred megahertz. Approximately one to two percent of the laser energy is absorbed by the electrons in a high efficiency cathode material. In an RF injector design, the ejected electrons are then accelerated up to approximately 5 MeV by RF energy within the injector assembly booster. The injector requires power input for the drive laser, RF energy, and cryogenic

cooling for the RF cavity. Vibrations at the injector can adversely affect the electron pulse leaving the cathode and disrupt the synchronism process.

The current planned shipboard FEL will use a recirculating superconducting LINAC to produce and sustain a relativistic electron beam. The LINAC receives 5 MeV electrons from the injector and uses superconducting RF cavities to accelerate them to about 100 MeV. LINAC modules require liquid helium cooling to reach superconducting temperatures and powerful next generation RF sources to reach the sustained power requirements of a mega-watt class FEL. Liquid helium requires a substantial array of cryogenic equipment and insulation to function. The ability of the cryogenic system to dissipate heat during continuous operation can be a limiting factor in the amount of time the laser can operate. The cryogenic refrigeration system must remove enough heat from the LINAC and injector assemblies to maintain superconducting temperatures. This can be accomplished by either employing a large enough refrigerator to remove a continuous operation heat load or a sufficiently large reservoir of liquid helium to allow extensive operation replenished by a less powerful refrigerator.

The electron beam is directed by magnets around an evacuated pipeline to the undulator. Dipole magnets are used for turning the beam and quadrupole magnets are used for beam conditioning. Beam position is managed by automated sensing and adjustment to beam line magnets at much higher frequency than shipboard vibration sources. The race track shape of the beam line and its relatively large diameter present an alignment challenge when subjected to large amplitude bending and torsional modes. If the beam pipe were misaligned beyond the capability of the magnets to correct the electron beam could strike the interior surface of the pipe preventing recirculation which would result in a shutdown of the entire system. Generation of the electron beam creates a halo of electrons outside the main beam. Poor beam alignment could allow interaction of the halo with the beam pipe resulting in heating, energy loss from the electron beam, and ionizing radiation. Additionally, results from NPS 3D FEL simulation code indicate that an uncorrected electron beam shift and/or tilt in the undulator, which could be caused by a misaligned magnet, would result in reduced extraction and overall laser power

output [1]. Electron beam alignment changes of milliradians in angle or millimeters in offset can dramatically affect FEL operation as shown in Figure 2.

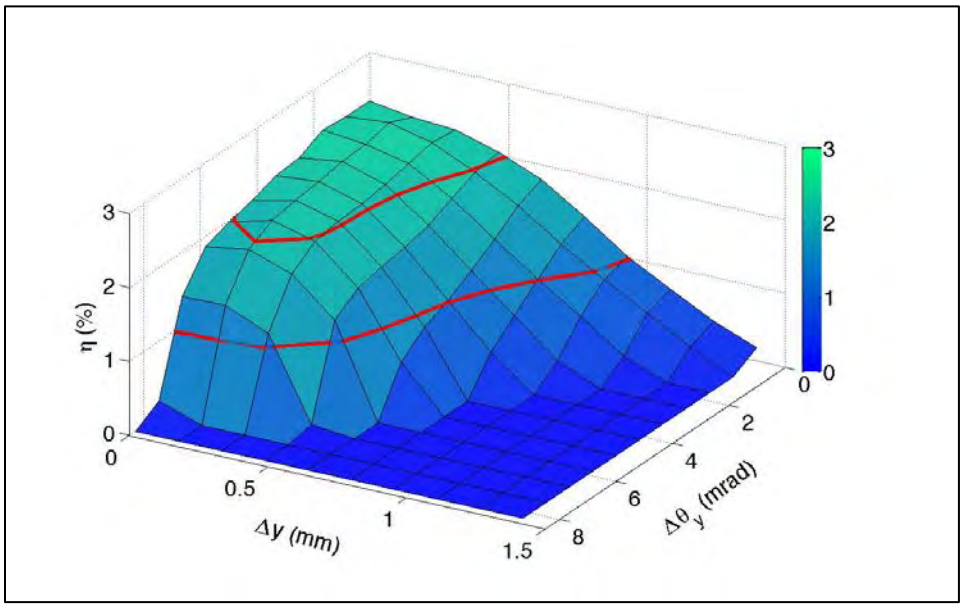

Figure 2. Optical Extraction (η) vs. Separation and Electron Beam Tilt for a Notional FEL Oscillator. (From [1])

The narrow beam pipe in the undulator requires a tighter tolerance on the electron beam than other components. The FEL interaction requires a precise control of the electron beam within the alternating magnetic fields. The undulator must also maintain precise alignment with the optical path determined by the tolerance of the resonator mirrors.

After passing though the undulator the electron beam returns to the LINAC module out of phase with the accelerating electromagnetic field. Energy from the electron beam is recovered to the field as the electrons decelerate and drop from approximately 100 MeV to 5 MeV. Using a recirculating electron beam for energy recovery allows a large fraction of the energy used to accelerate the beam to be recovered.

The remaining lower energy electrons are guided into the beam dump. The electrons entering the beam dump at approximately 5 MeV and 1 A generate 5 MW of

heat that must be dissipated through water cooling. The beam dump is constructed from a large block of copper for its high heat capacity and thermal conductivity. The water cooling system that the beam dump requires is a source of vibration that must be decoupled from the FEL. Figure 3 is a top down view of the entire electron beam path.

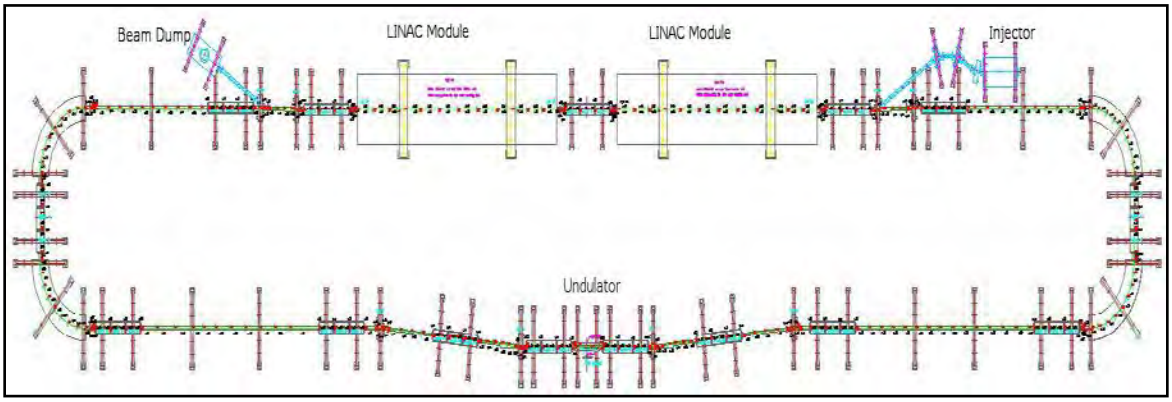

Figure 3. Electron Beam Line of a Notional FEL Oscillator.

2. Optical Path

The optical path between the mirrors is the portion of the FEL most susceptible to misalignments. The mirrors must maintain a separation within a tolerance of micrometers and an angular alignment within microradians for the laser to operate. The need to align the mirrors to high tolerance conflicts with the necessity of spacing them far apart to allow the optical beam to diffract enough to prevent damage to the mirrors due to heating.

It is anticipated that on a ship an active control systems will be required for each end of the optical path to maintain alignment. The response range in amplitude of such precise systems is limited, so that passive control measures will need to be applied to reduce the amplitude of vibrations transferred to the mirrors.

3. Shipboard Installation

Currently all FELs are constructed in a laboratory setting and the transition to a shipboard system presents numerous challenges. All shipboard systems compete for limited space and must be made as compact as possible. Currently the world's most

powerful FEL at Jefferson Lab has a footprint of nearly 900 m^2 [2], a shipboard installation must be seventy times more powerful and fit in a footprint of roughly 150 m^2.

The shipboard FEL will be exposed to an environment fraught with both sustained and unpredictable sources of vibration. Sustained vibrations arise from the pressure effects of propulsion on the hull and collocated machinery. Wave-action induces large amplitude low frequency motion in pitch and roll to the hull which must be decoupled for the FEL to allow operation. The FEL may pitch and roll with the hull of the ship and a beam director topside is used to maintain laser power on target.

Current shipboard vibrational testing standards are dictated by MIL-STD-167-1A [3], which dictates subjecting shipboard equipment to excitation from 4 to 33 Hz with amplitude up to 0.030±0.006 inches. This test simulates only propulsion derived excitation. A separate simulation of hull motion in various sea conditions was conducted using SHIPMO software to determine excitation based on free body hull motion due to wave action.

The influence of surrounding equipment on the FEL is determined by examining the mode shapes of the system and comparing the frequencies that they occur with the operating frequencies of surrounding equipment. Connections to support equipment required to operate the FEL provide conduits for vibrational excitation that are challenging to suppress.

D. SCOPE OF RESEARCH

1. Vibration Simulation

This project uses a notional model of a shipboard FEL oscillator to determine the nature of vibration induced motion in the system. The data from the model is used to determine areas of the FEL that are outside the system's vibrational limits and must be actively controlled to operate. Vibration transmitted due to hull excitation from wave action and underwater explosion are investigated.

2. Passive Control Solutions

Passive control mechanisms use systems of mass, stiffness, and damping to reduce the undesirable effects of vibration. The modeling control systems as functions of mass, stiffness, and damping allows simulation solutions for vibration control which can be correlated to real world devices with as near as practical identical properties. One objective of this project is to determine the shipboard vibration environment and what control measures are required to operate a notional FEL weapon system on board a ship.

3. Electron Beam Path Components

After developing a method for modeling the system and its vibrational inputs special attention is given to the resulting motion of components that comprise the electron beam path. It is assumed that active electron beam steering controls will be used and the key research is the nature of the residual motion that will be passed on from passive control measures. Sources of distortion due to component layout in the electron beam path are also sought in order to improve future FEL configurations.

THIS PAGE INTENTIONALLY LEFT BLANK

II. CAD MODEL DEVELOPMENT

A. MODEL CONCEPT

The model developed for this research is based on a notional configuration of a production shipboard FEL oscillator rather than the Innovative Naval Prototype. Dimensions of the FEL were constrained by the distance required between the mirrors, the length of the LINAC units, and a turn radius of one meter for the electron beam. The installation was assumed to be in a single compartment similar to a current shipboard auxiliary space where the FEL is affixed to a shock mounted foundation to provide stiffness and reduce relative motion between components while preventing transmission of hull excitation to the system.

B. SOLID MODEL

1. Development

A Computer Aided Design (CAD) model developed for the shipboard FEL was first constructed in Solidworks based on components of the Stanford University FEL, and is shown in Figure 4. Components were developed to represent a reasonable approximation of geometry, location, and material properties.

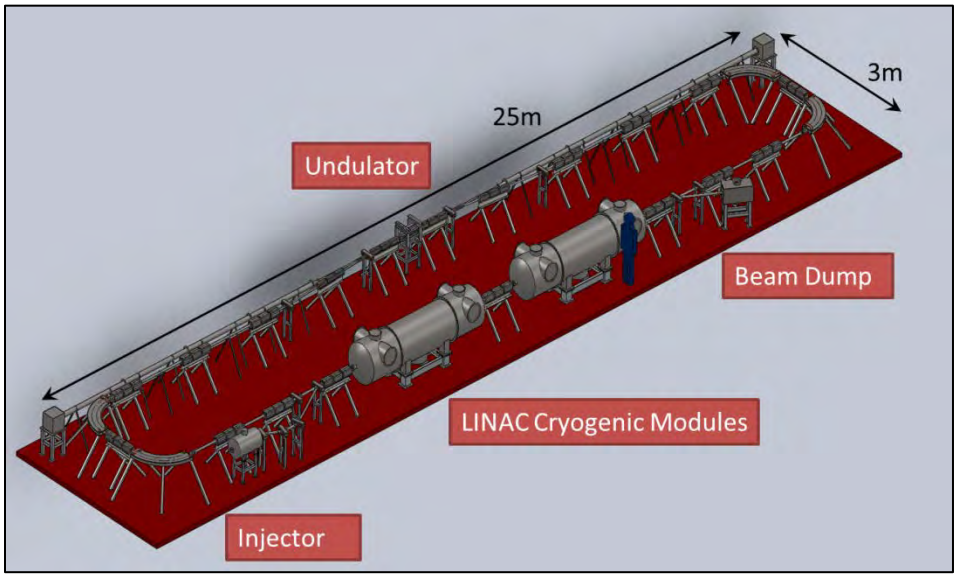

Figure 4. Solid Model of a Notional Free Electron Laser

Geometry and material properties of the equipment are essential for developing accurate moments of inertia and cross-sectional areas required for estimated stiffnesses used in simulation. Correlation between the mass of model components and masses of components predicted by Advanced Energy Systems FELSIM software [4] was used to check the realism of individual components. Stainless steel was selected for the majority of components in keeping with current laboratory equipment. All magnets with the exception of the rare earth magnets in the undulator were modeled as electro-magnets constructed from copper in a steel assembly. The injector section of the model shown in Figure 4 is a simplified version of a superconducting model developed by Niowave Inc. [5].

2. Assumptions

FEL operation requires a significant quantity of support equipment and services. Auxiliary equipment such as RF sources, electric power, cryogenic refrigerators, and cooling water is assumed here to be decoupled in vibration from the electron beam path and optical path of the FEL. Simulations of final FEL designs must incorporate the equipment noise as the auxiliary configuration becomes known.

The optical path for the FEL solid model was developed under the assumption that an active control system would be required to maintain mirror alignment. The active control system is modeled as a "black box" with a mass to approximate the weight of a mounting system, control servos, and cooling equipment.

3. Mounting Considerations

The FEL's connection to the ship in the solid model uses a baseplate simulating the type of foundation currently used by auxiliary equipment. The height of the beam line is determined by the clearance required for the LINAC modules, including clearance to allow for RF connections on the bottom. Quadrupole magnets are mounted in sets of three on an I-beam base with box cross-section legs. The injector, beam dump, LINAC units, and mirror units are mounted on individual frames made of box-section steel. The undulator is mounted in a framework of I-beams to contain the strong magnetic forces of the rare earth magnets.

C. BEAM MODEL

1. Development and Assumptions

In simple geometry systems such as a cantilever beam, determining displacement and resonant frequencies is a relatively simple hand calculation. However, the complex geometry of the FEL system requires advanced modeling and solving techniques in simulation. Yet, the solid model developed in Solidworks is too complex and detailed to be efficiently used in simulation directly. A compromise is to use a less complex model that represents the pertinent properties of the solid model. It must be solved numerically to extract representative motion data while running in a reasonable amount of time on ordinary hardware.

The mass and stiffness of FEL components and the points where they join together must be accurately represented by the simplified model. A "beam model" is the simplest model type that is sufficiently accurate. Top view cut-away drawings extracted from the solid model were used to map the geometry for the beam model as an array of "node" points in several layers. ANSYS beam elements were constructed between nodes within and across layers to represent the geometry of the FEL, and shell elements were used to represent the baseplate on which it is mounted.

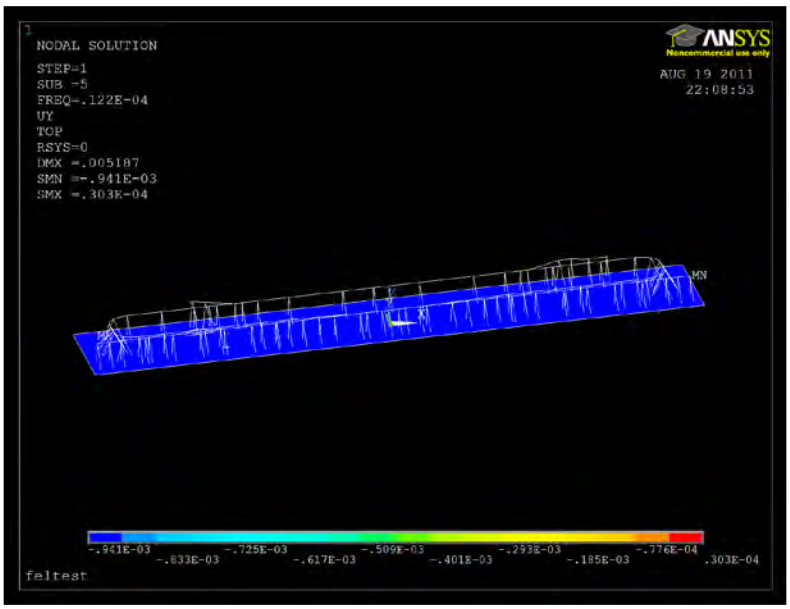

Figure 5. Isometric View of the FEL Beam Model Derived from the Solid Model

Each beam element in the model requires a unique set of physical properties to properly represent the components of the solid model. Cross-sections of each solid model component type, as demonstrated in Figure 6, are used to calculate the geometry based physical values required for the beam model. Many other components were modeled in order to capture their mechanical properties in the beam model.

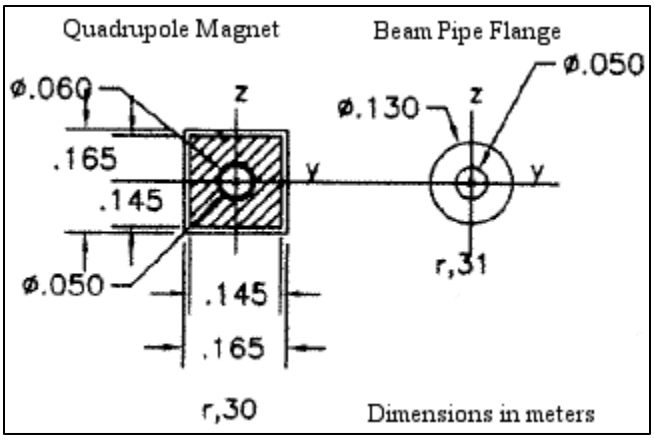

Figure 6. Examples of Component Cross-sections

The second moment of area, also known as the area moment of inertia, is an important characteristic in determining how components are likely to deflect under loading. It is an example of the geometric properties derived from the solid model cross-sections essential to construct the beam model elements. A sample calculation of the second moment of area for the circular beam pipe flange from Figure 6 is given by equations 1–3:

component type. These unique sets of characteristics are then applied to each beam element in the model.

The shell elements used to create the base plate are given the material properties of steel and geometric properties defined in ANSYS. The density of the base plate was initially reduced to 25 percent of ordinary steel to represent a structure of I-beams with a stiffness equivalent to the solid slab of steel modeled in ANSYS. The thickness of the baseplate was selected such that the first bending mode with free ended constraints would occur around 10 Hz, well above the frequency of ground excitation due to ship motion and an order of magnitude separation from the natural frequency of the planned shock mounts

2. Mounting Considerations

The FEL beam model uses the baseplate as the support structure on which the electron beam and optical paths are mounted. Simulating ground excitation due to ship's motion requires the development of a framework of near infinite stiffness and negligible mass beams attached to a point mass at which excitation is applied. Choosing a mass 1000 times greater than the mass of the system prevents the model from influencing the motion of the ground, in this case representing the ship's hull. The low-mass high-stiffness beams transmit the motion to the points where the model is connected to the hull without deflection. The FEL beam model is attached to the excitation framework through ANSYS COMBIN14 elements which simulate stiffness.

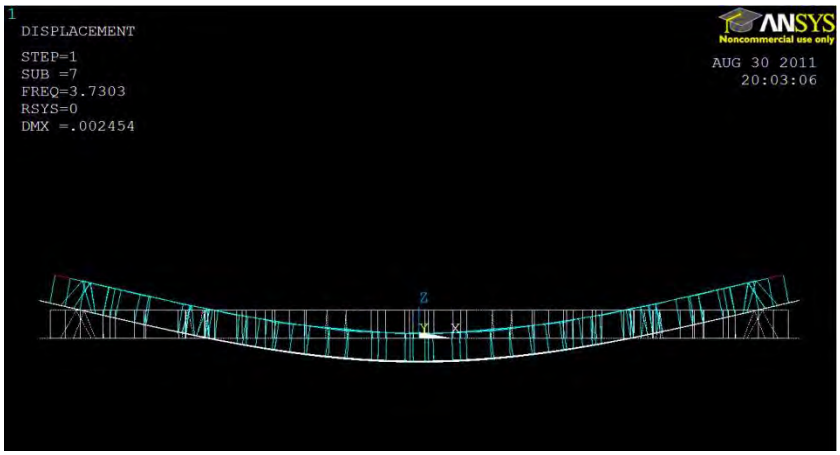

Figure 7. Example Free-Free First Bending Mode Shape Side View Used To Develop Spring Mount Locations.

The ideal mounting points to connect the framework and baseplate are locations of minimal motion. A mode shape analysis of the FEL mounted on the base plate with free-free end constraints was used to determine the node lines of the first bending mode, as shown in Figure 7. Typically, the first bending mode has the highest vibration amplitude after the basic translations and rotations. The FEL is not symmetrical about any axis due to the optical beam piping on the undulator side of the electron beam path and the difference between the beam dump and the injector on the LINAC side. The lack of symmetry in the FEL system model generated a minor torsional distortion in the first bending mode, but it was negligible in determining the mounting points. Four connections to the excitation frame were arranged in a rectangular pattern along the vertical axis below the base plate at either end of the node lines for the first bending mode. Three additional COMBIN14 elements were added in the horizontal plane, two parallel to the y-axis and one along the x-axis to control motion along those axes as shown in Figure 8.

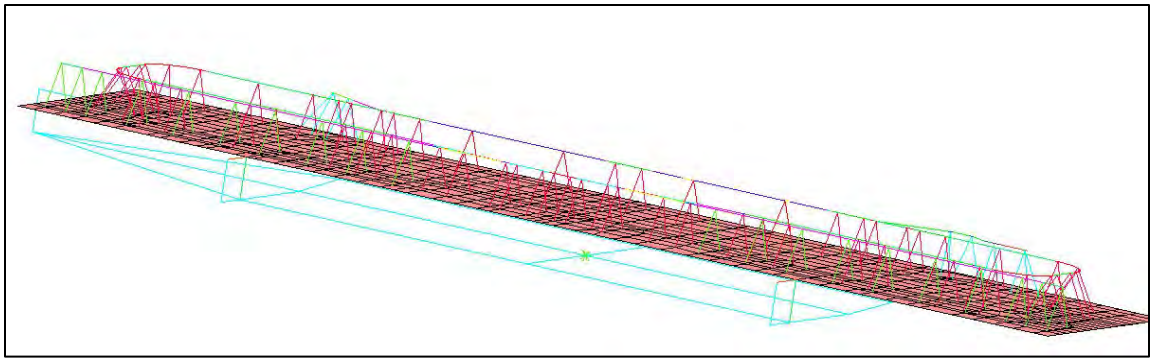

Figure 8. FEL Beam Model With Base Excitation Framework in Blue

The FEL beam model shown in Figure 8 was shock mounted at 1 Hz according to the equation,

THIS PAGE INTENTIONALLY LEFT BLANK

III. SIMULATION METHOD

A. FINITE ELEMENT ANALYSIS

The Finite Element Method (FEM), or Finite Element Analysis (FEA), is a numerical procedure for solving partial differential equations to determine the normal modes of the FEL system model. Applying FEA to a system requires that the model be discretized into individual elements. The FEL system beam model was developed specifically to allow for rapid FEA using ANSYS by using as few elements as required to sufficiently represent the system.

B. ANSYS

The FEL Beam model was developed and initially evaluated in ANSYS [6]. The motion of components is followed by the motion of critical node points. Each node point is free to move in the six primary degrees of freedom (DOF), three translations and three rotations, subject to the constraints of its connections to other components. The motion of each node is related to the motion of adjacent nodes through coupled partial differential equations. The block Lanczos method [7] of finite element analysis is used to solve for the frequencies (eigenvalues) and mode shapes (eigenvectors) for all DOF of the model. Figure 9 is an example of the solved eigenvector output for several nodes corresponding to beam line elements across all six DOF at the 1.0839 Hz eigenvalue.

```
MAXIMUM ABSOLUTE VALUES
NODE     102850      102850      100032      100650         260      100016
VALUE   0.73140E-02 0.10860E-01 0.14273E-01 0.15517E-03 0.22586E-03 0.42530E-03

 ***** POST1 NODAL DEGREE OF FREEDOM LISTING *****

 LOAD STEP=     1  SUBSTEP=     5
  FREQ=    1.0839      LOAD CASE=   0

 THE FOLLOWING DEGREE OF FREEDOM RESULTS ARE IN THE GLOBAL COORDINATE SYSTEM

   NODE      UX          UY          UZ          ROTX        ROTY        ROTZ
      4  0.62375E-02 0.10170E-01 0.80775E-02 0.14846E-03 0.22183E-03 0.41864E-03
     16  0.60952E-02 0.10170E-01 0.81280E-02 0.14825E-03 0.22188E-03 0.41864E-03
     36  0.58981E-02 0.10162E-01 0.82020E-02 0.14803E-03 0.22210E-03 0.41843E-03
     48  0.56827E-02 0.10047E-01 0.83393E-02 0.14786E-03 0.22205E-03 0.41847E-03
     60  0.55676E-02 0.98315E-02 0.84941E-02 0.14772E-03 0.22189E-03 0.41852E-03
    140  0.55607E-02 0.85329E-02 0.91856E-02 0.14768E-03 0.22306E-03 0.41870E-03
    152  0.55607E-02 0.83905E-02 0.92613E-02 0.14765E-03 0.22267E-03 0.41867E-03
    164  0.55607E-02 0.82482E-02 0.93371E-02 0.14762E-03 0.22301E-03 0.41875E-03
    180  0.55608E-02 0.81100E-02 0.94107E-02 0.14759E-03 0.22361E-03 0.41885E-03
    216  0.55715E-02 0.77755E-02 0.95857E-02 0.14780E-03 0.22409E-03 0.41871E-03
    236  0.55716E-02 0.76384E-02 0.96592E-02 0.14786E-03 0.22447E-03 0.41900E-03
    248  0.55716E-02 0.74959E-02 0.97356E-02 0.14801E-03 0.22518E-03 0.41940E-03
    260  0.55716E-02 0.73533E-02 0.98123E-02 0.14815E-03 0.22586E-03 0.41961E-03
    296  0.55716E-02 0.69185E-02 0.10046E-01 0.14915E-03 0.22543E-03 0.41901E-03
    308  0.55716E-02 0.64516E-02 0.10297E-01 0.14918E-03 0.22523E-03 0.41909E-03
```

Figure 9. Example of DOF Eigenvector Output for 1.0839 Hz. UX, UY, UZ, ROTY, ROTX, and ROTZ Represent the Primary Translations and Rotations.

Eigenvalue output form ANSYS is exported to MATLAB to build the vibration simulation for the FEL system. The acceleration that will be applied to the model must be determined prior to running the MATLAB simulation of FEL system motion. Ship motion simulation software is used to simulate the rigid body motion of the hull to which the FEL system is mounted.

C. SHIPMO

SHIPMO [8] is a program which calculates the frequency domain motion of a hull in a simulated sea state. A destroyer hull form was selected for analysis as it is the smallest hull form likely to support an FEL system and would be more susceptible to wave action induced rigid body motion when compared to larger hull forms. Waves in the simulation are defined by wavelength and output motion amplitude is a unit-less multiple of any desired input wave height. SHIPMO was used to evaluate the rigid body

motion of the hull which is dependent on the bearing of the incident waves and the speed of the ship. Waves are simulated across incident bearings from zero to 180 degrees in 15 degree increments for hull speeds from 0 to 15 meters per second in 1 meter per second increments. Hull speeds in excess of 15 meters per second, about 30 knots, are not sustainable in significant seas by current destroyer hull forms, and as such were neglected.

Data from the SHIPMO simulation is processed in MATLAB to determine RMS values for rigid body hull motion across various Douglas Scale [9] sea states as defined by the World Meteorological Organization (WMO). Douglas Scale sea state is a ten tier system based on the significant wave height in ocean waves as shown in Table 1.

WMO Sea State	Average Significant Wave Height (m)	Wave Characteristics
0	0	Calm (glassy)
1	0.1	Calm (rippled)
2	0.4	Smooth
3	1.1	Slight
4	2.4	Moderate
5	3.5	Rough
6	5.5	Very Rough
7	8.0	High
8	12	Very High
9	14+	Phenomenal

Table 1. World Meteorological Organization Sea States (From [9])

Data for each sea state, bearing and speed are used to generate polar plots of pitch, roll, vertical acceleration, lateral acceleration, and slam acceleration and velocity. Absolute vertical acceleration is used as the excitation in the MATLAB based FEL system model, where the FEL is assumed to be located near the pitch and roll centers of the ship to minimize the effects of slam and lateral acceleration. Sea state six was assumed to be a

reasonable limit for normal combat operations as higher seas and associated weather would likely impede target detection and tracking. Vertical acceleration in g for sea state six is given in Figure 10, where speed increases from 0 to 15 m/s from the center to the edge of the plot and bearing is the relative heading difference between the ship and the waves. The period of excitation for sea state six, given in Figure 11, is also extracted from the SHIPMO simulation and used to determine the frequency of hull excitation to apply to the model.

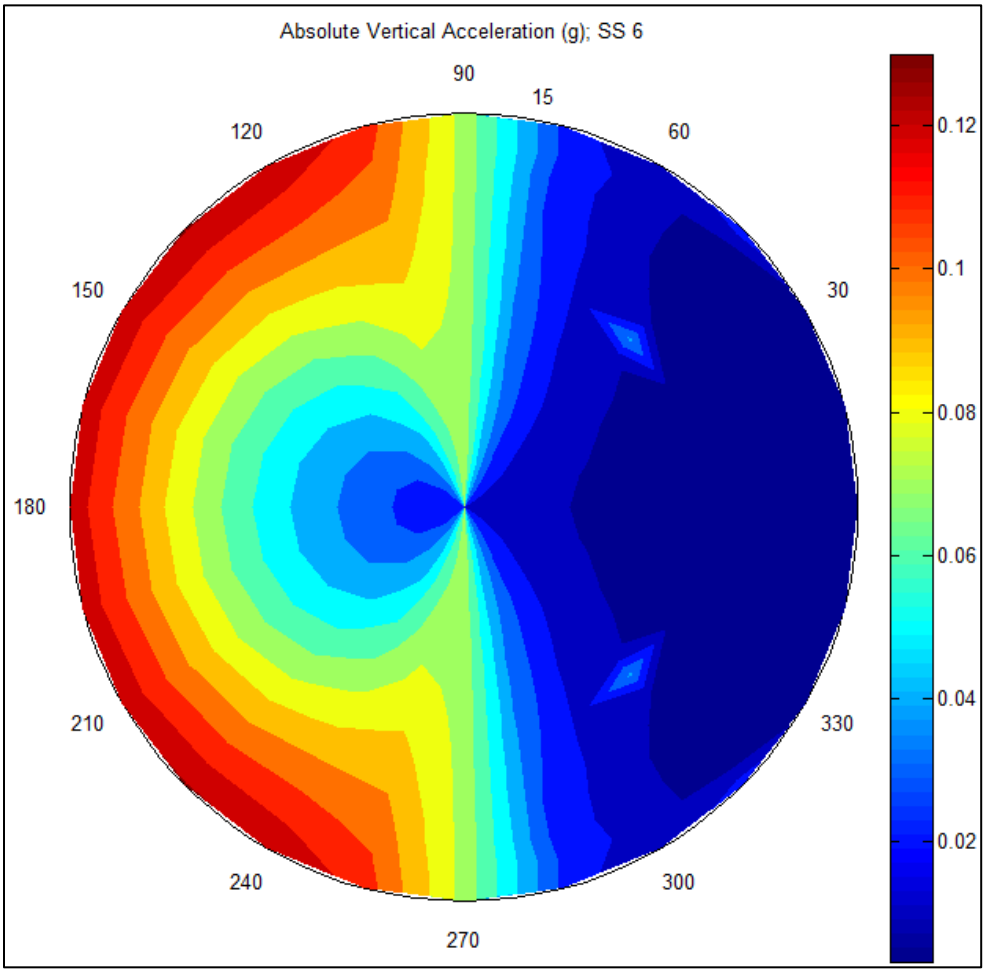

Figure 10. Sea State Six Vertical Acceleration vs. Speed and Heading. Ship's Speed Increases Radially 0 to 15 m/s from the Pole to the Outside Edge.

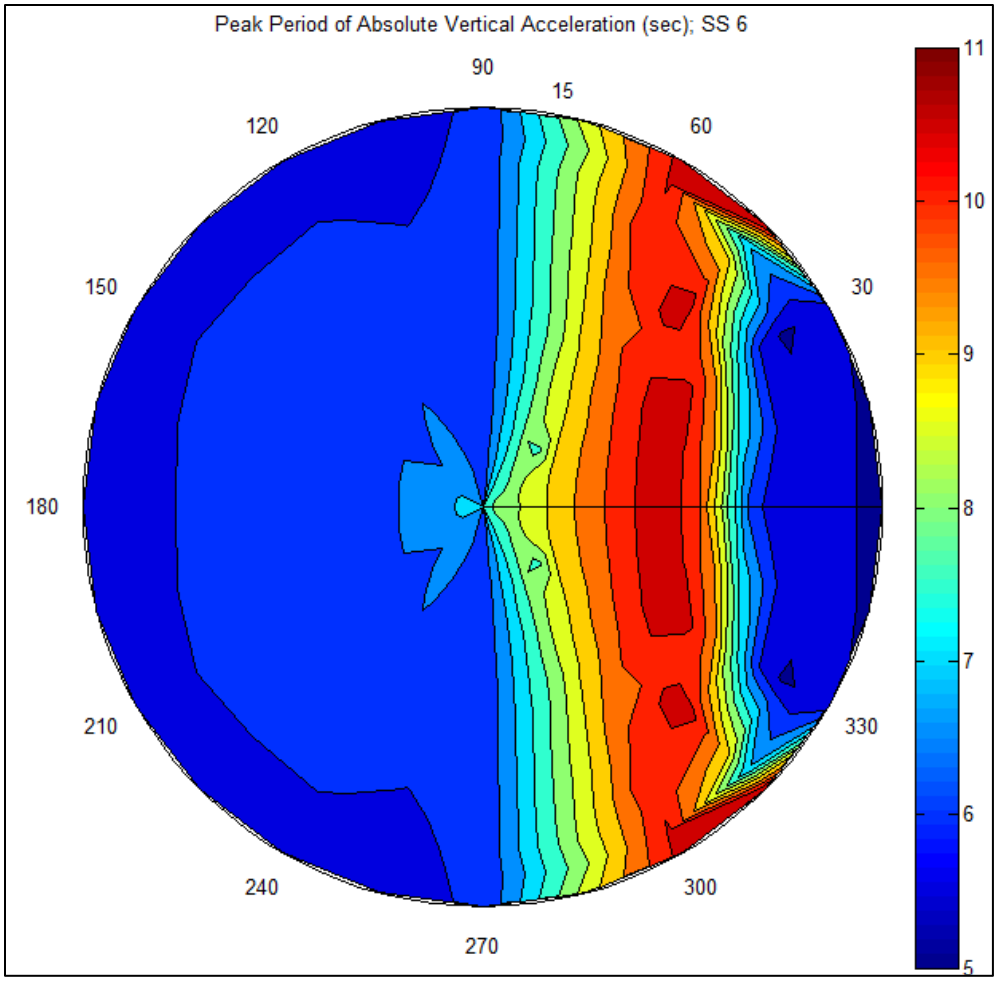

Figure 11. Sea State Six Oscillation Period vs. Speed and Heading. Ship's Speed Increases Radially 0 to 15 m/s from the Pole to the Outside Edge.

D. UNDERWATER EXPLOSIVE SHOCK INPUT

Mounting the FEL system on a warship exposes it to the possible vibration effects of underwater explosions. Surface ships are currently subjected to shock trials in accordance with NAVSEA 0908-LP-000-3010A [10], where acceleration data is collected from hulls exposed to controlled close aboard underwater explosions. Test data (Figure 12) from the shock trials of USS Winston Churchill (DDG-81), a DDG51 class hull form, was used to generate a shock pulse input for the FEL system model. The peak acceleration in g and the initial shock pulse width are applied as a half sine pulse. The data measured by an accelerometer mounted in an auxiliary space best represents the probable location of the FEL system, in this case, an auxiliary machinery and pump room

was selected. The first impulse of the shock trial acceleration data was approximated as a half sine wave pulse and used to represent underwater shock input for this experiment.

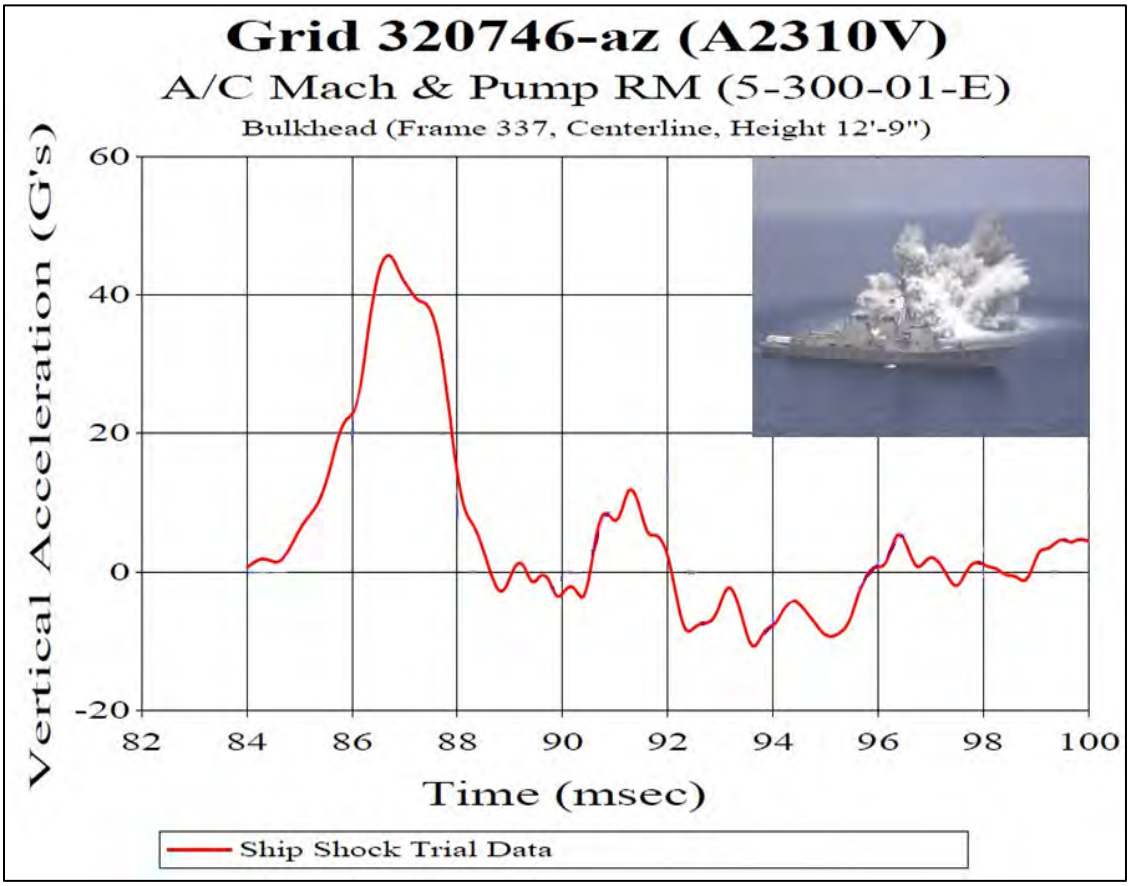

Figure 12. DDG 81 Shock Trial Data. (After [11])

E. MATLAB

1. State Space Model

State space form is used to represent a multiple degree of freedom (MDOF) system defined by n second order differential equations as a system of $2n$ first order differential equations in a principal coordinate system to allow rapid numerical solutions to be calculated [12]. In the principal coordinate system, the variables are the displacements and velocities of each mode rather than those of physical objects. The modal analysis eigenvector output from ANSYS is imported to create a state space model in MATLAB. The normalized eigenvector output is used to transform the forcing

functions and initial conditions to the principal coordinate system to yield a solution. The physical coordinate solution is developed by back transforming from principal coordinates in a manner analogous to inverting a Laplace transform. Creating a state space model in MATLAB allows frequency and time domain responses to be calculated for the FEL system simultaneously [12].

2. Excitation Implementation

The acceleration data extracted from SHIPMO is applied to the model through the use of a continuous sine wave with an amplitude of 0.12g and at a frequency of 0.2 Hz generated by the hull's rigid body motion. The input, shown in Figure 13, is applied to a point mass in the ground excitation framework of model to simulate a hull which transmits the force through shock mounts to the FEL system. Simulating an underwater explosive vibration input is done in the same manner by replacing the continuous sine with a half sine pulse with a peak amplitude of 45g and a period of 4 milliseconds derived from shock trial data.

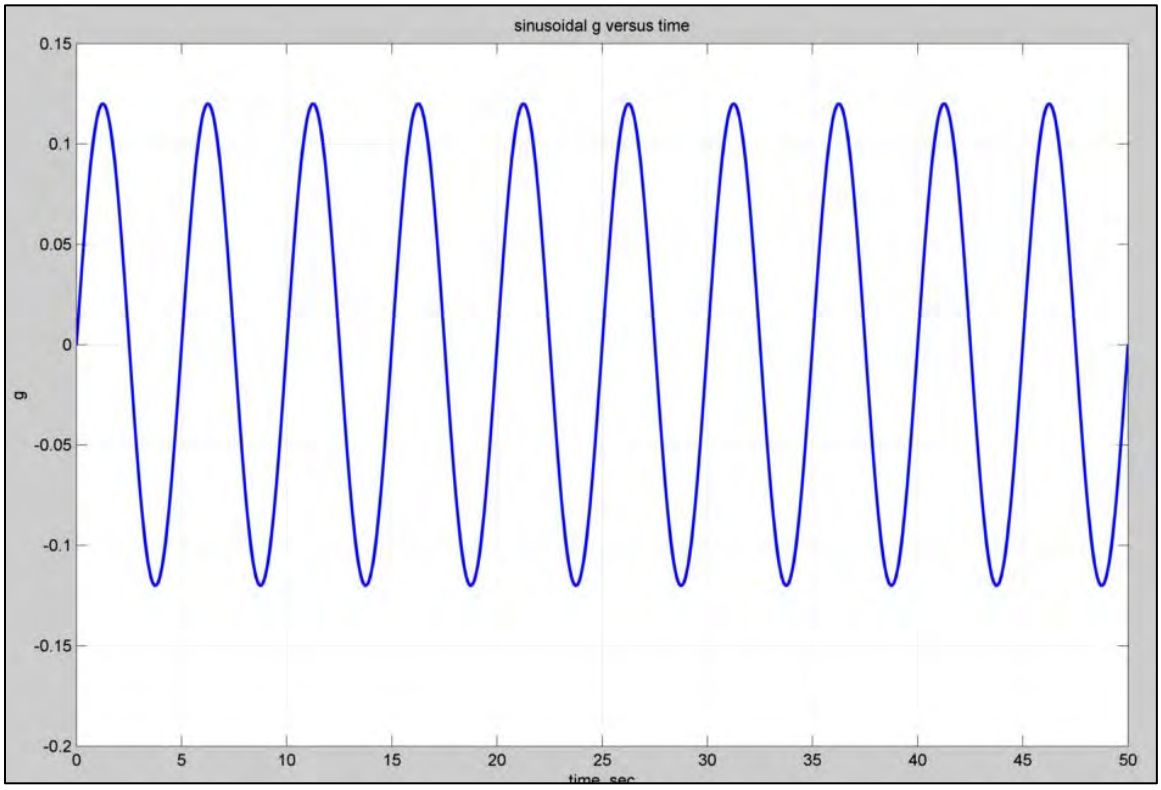

Figure 13. Steady State Wave Driven Continuous Sine Input

3. Output

The MATLAB model solution outputs modal contributions to the transfer function of each degree of freedom. The frequencies that will excite modes of individual components can be observed easily as peaks in the modal contribution graph, such as Figure 14. The blue line in Figure 14 is the summation of all the black line modes. In addition to the modal contributions, MATLAB is also used to generate plots of physical displacements of individual components in time domain spatial coordinates. The alignment between components can be determined by calculating the difference in their respective displacements within the spatial plane of interest.

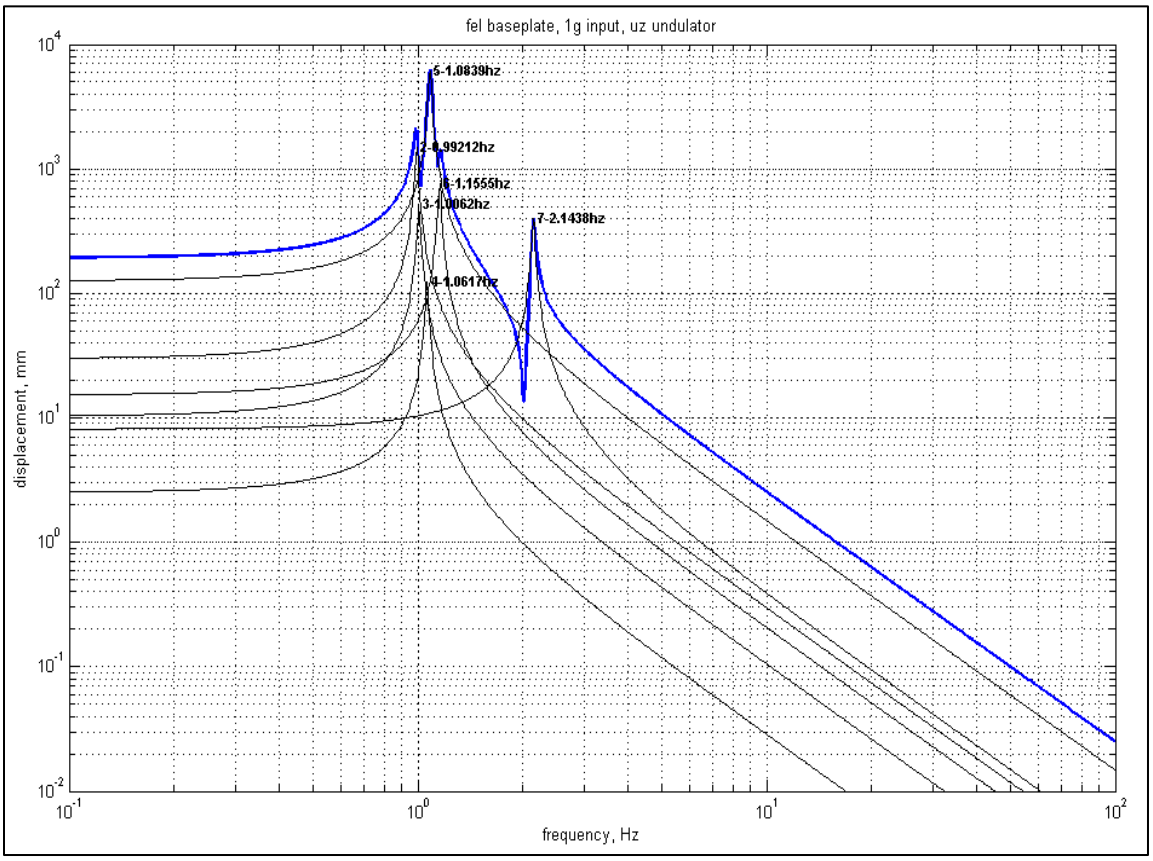

Figure 14. Modal Contribution Plot Example: Undulator in z-direction

F. ITERATION

Optimized passive controls for the FEL system must be implemented over many iterations of the simulation process. Information from the modal contribution graphs of

components of interest is used in conjunction with the corresponding ANSYS mode shape animations to identify elements of the model that require additional vibration reduction measures. Adjustments to the baseplate, shock mounts, and component mounting brackets can be tested and evaluated through iteration of the simulation process. The end goal of the simulation process is to develop a model of passive controls which minimizes misalignments in the FEL system by reducing the displacement amplitudes of important components.

THIS PAGE INTENTIONALLY LEFT BLANK

IV. TESTING

A. PRELIMINARY ISOLATION CONCEPT

The shipboard vibration environment dictates the nature of isolation that must be applied to the FEL system to allow it to operate. Separation between the frequency of excitation and the mechanical oscillation frequency of FEL system is required to prevent excitation of component normal modes with high amplitudes of displacement. Table 2 illustrates the range of excitation frequencies that the isolation system for a shipboard FEL system must handle.

Source	Frequency Range
Wave Motion- Rigid Body	0.5 Hz and below
Propulsion [3]	4 to 33 Hz
Operating Equipment	10's to 100's of Hz
Underwater Explosions	Up to 100's of Hz

Table 2. Excitation Sources Requiring Isolation

Placing the sensitive components of the FEL system on a platform isolated at a natural frequency that is separated from the frequencies of excitation significantly reduces the transfer of hull vibrations to critical components. The frequencies of the platform's normal modes must also be separated from the natural frequency of the entire system riding on its isolating springs. The initial passive isolation system was designed for an isolation frequency of one Hz to take advantage of the frequency gap between wave motion and propulsion driven excitation. The initial platform was developed to have its first bending mode at 10 Hz to provide roughly one decade of separation from the isolation frequency of one Hz. Only passive control measures were considered to determine the nature of the resulting motion which may or may not require active control measures depending on the tolerances of individual FEL system components.

B. MODEL IMPROVEMENTS

1. Component Stiffening

Initial observation of mode shape animations in ANSYS revealed excessive motion of several FEL system components. Motion of heavy components, such as the injector and the beam dump, was transferred to the attached beam pipe and induced a torsional motion around the entire electron beam path. Additional supports were attached to the beam dump and injector in the beam model and mode shapes were re-evaluated. Additionally, "jump rope" mode shapes were observed along the optical pipe between the mirrors and corrected with additional supports. While these specific corrections only apply to the notional FEL model, the methodology of observing mode shapes to develop improved component mountings should be applicable to future models.

2. Box Platform Model

In order to achieve finer control over the mass of the FEL system, which is predominantly comprised of the mounting platform, the reduced mass plate was replaced with a three dimensional platform assembled from ANSYS shell elements. The platform was constructed by sandwiching a boxed rib structure between a series of plates. An iterative algorithm for modifying the platform material geometry and evaluating the first bending mode, first torsional mode, and FEL system mass was developed in ANSYS and used to find the optimal platform dimensions for high stiffness at the lowest possible mass. Aluminum was selected as the material for the platform for its low density. The thickness of the box, and the plates it was constructed from, were modified and tested. Figure 15 illustrates the frequencies of the first bending mode and first torsional mode in Hz versus the resulting overall system mass in kg that resulted from changes to the top and bottom plate thickness and the thickness of the internal rib structure.

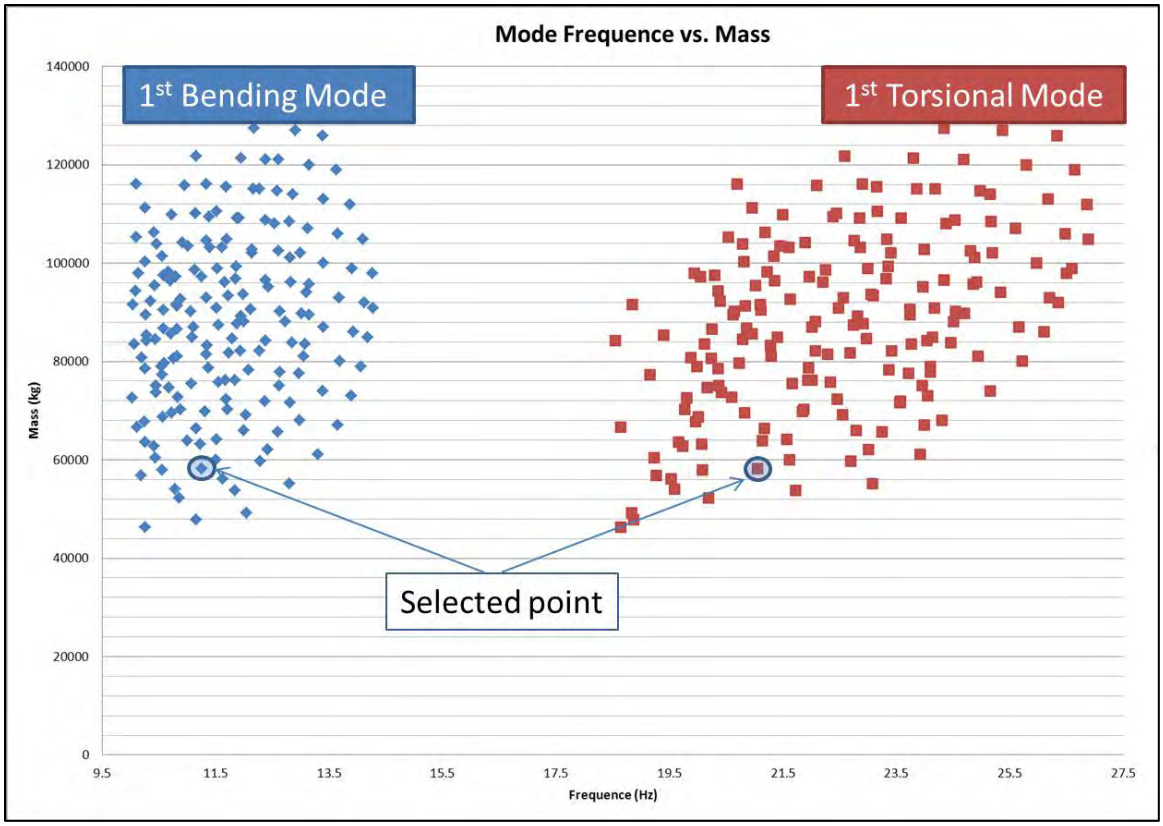

Figure 15. Bending and Torsional Frequencies of Box Platforms vs. Mass

Optimization to reduce the mass of the platform resulted in an excessively thin top plate that allowed motion of heavy FEL components due to surface deflection. The minimum plate thickness to prevent surface mode shapes at a lower frequency than the first torsional mode was found to be 5 cm. The optimal platform mass of 58 metric tons for a 5 cm plate thickness has a first bending mode of 11.43 Hz and first torsional mode of 21.13 Hz with a box thickness of 80cm and rib thickness of 2 cm. Figure 16 is an illustration of the internal structure of the platform and Figure 17 depicts the final platform design with the FEL system installed.

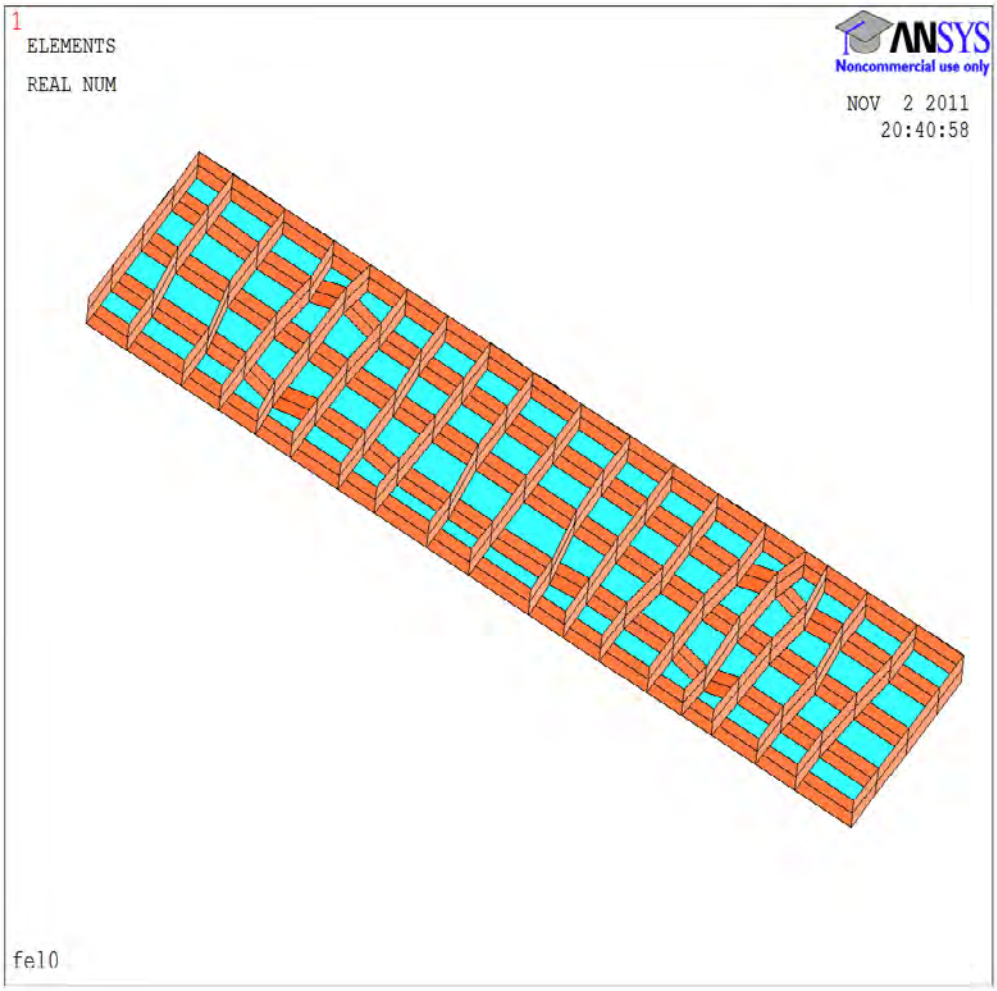

Figure 16. FEL Platform Showing Internal Rib Structure Configuration

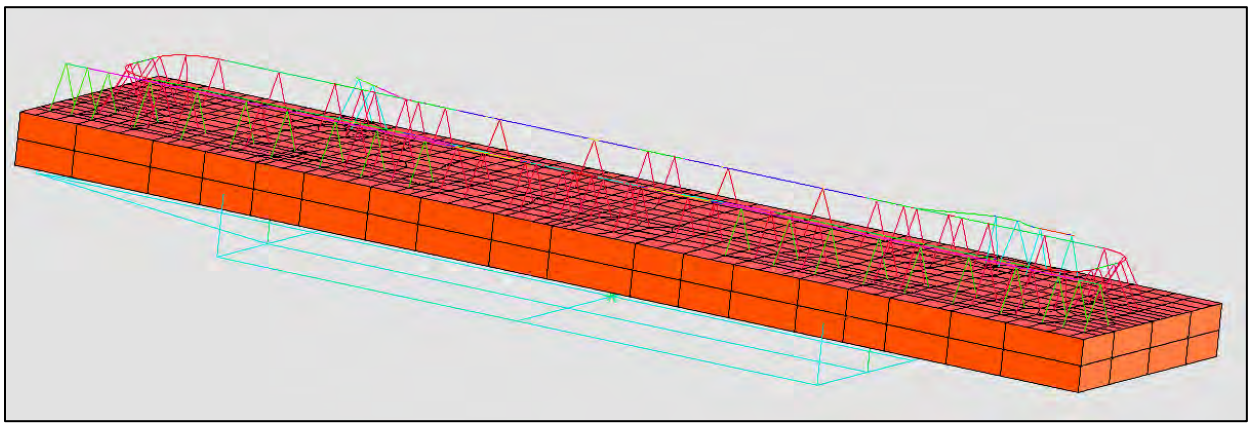

Figure 17. FEL Boxed Platform Model

3. Realistic Spring Implementation

Reducing the mass of the platform reduces the number of springs required in the one Hz isolation system by reducing the static load of each spring. Isolation springs in the model represent linear springs which adhere to Hooke's law and as such the spring rate for one Hz isolation is proportional to the sprung mass, which is the total mass that must be supported by springs. Reducing the sprung mass of the system allows for a lower spring rate and more easily produced real springs. The uneven distribution of mass due to the weight of electron beam line components developed a roll motion about the long axis. Countering this roll motion required an uneven distribution of vertical isolation springs, as shown in Figure 18, where five of the nine vertical isolators are placed on the LINAC side of the FEL system.

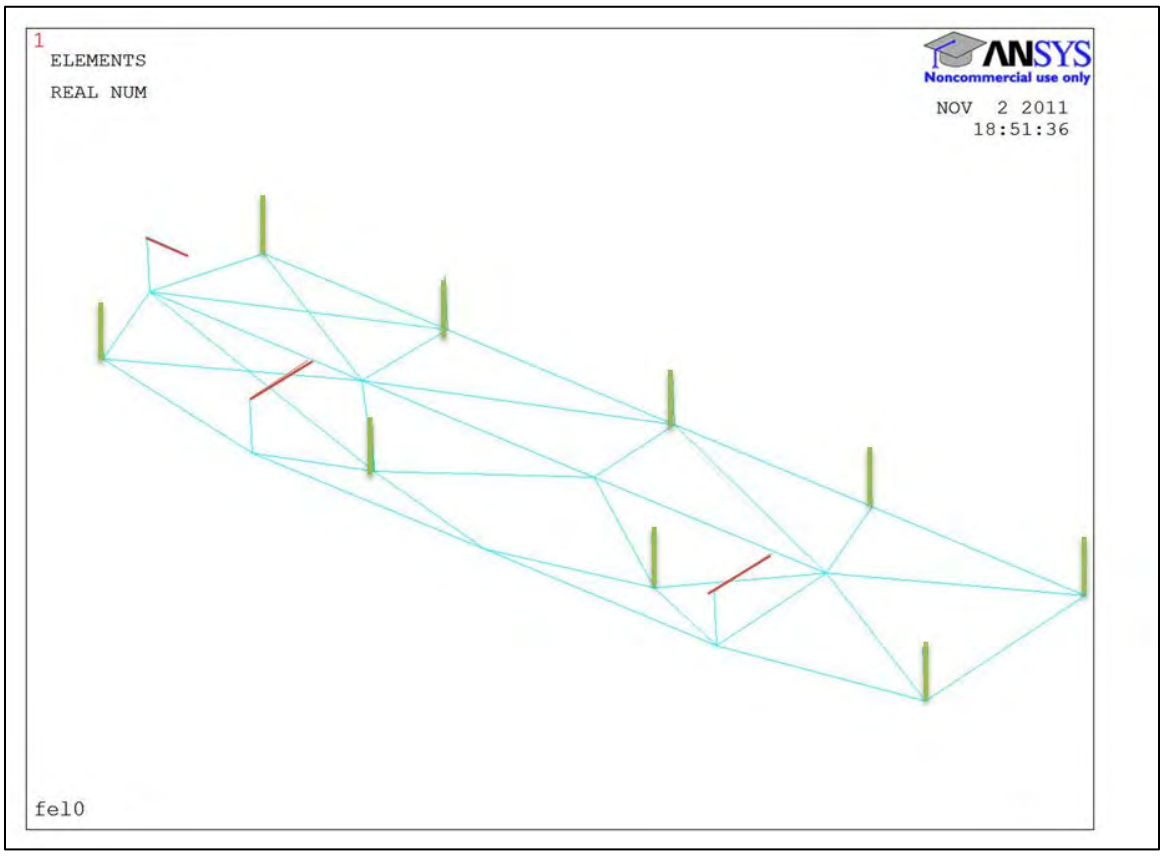

Figure 18. Twelve Spring Isolation System

Air springs produced by Firestone [13] with a maximum static loading of 13.6 metric tons per spring and adjustable stiffness were suggested for use by Senior Engineer Michael Evert of CSA Engineering of Mountain View, CA [14], whose company used similar components for the passive elements of the optical bench for the Air Force's Airborne Laser [15]. Air springs are a widely used technique to isolate equipment at low frequency. Air springs behave as an ideal spring within a specified range of deflection beyond which stiffness increases non-linearly. Modeling the isolators as linear springs is reasonable with the understanding that under extreme loading, displacement amplitudes would be reduced and the isolation frequency would intermittently increase until displacement damped into the linear range. The maximum vertical displacement of the platform observed under steady state wave excitation was ±3 centimeters from the static loading zero point, well within the range of linear behavior. The maximum displacement of the platform for an underwater explosive shock input was ±15 centimeters from the static zero point, which may exceed the linear behavior region of a given air spring depending on design.

C. ELECTRON BEAM PATH

A large disparity in the mass of individual components is inherent in the design of the FEL system electron beam path. Massive components such as the injector assembly, LINAC modules, undulator, and beam dump must be connected through the considerably lighter beam line, itself interspersed with moderately massive beam steering magnet assemblies. The FEL interaction generating the laser light in the optical resonator is dependent on bunches of electron navigating the electron beam path with precise timing. Any deformation of the beam path due to vibration must be accounted for by electron beam controls. The accuracy of any motion simulation is dependent on the accuracy of the model and the inputs. In this case, the order of magnitude of the motion is the significant data until a better concept FEL system model is developed.

1. Injector Assembly

The injector assembly in this FEL model is based on one developed by Niowave Inc. as an experimental superconducting model [5]. The electron beam travels from its

origin in the injector through a series of four dipole magnets to merge into the "racetrack" prior to entering the LINAC: The motion of the injector assembly and magnets relative to the merge point of the electron beam path is of interest in order to assure that timing of the electron bunches into the LINAC module is sufficiently accurate. Figure 19 is an illustration of the injector assembly and path into the main beam path.

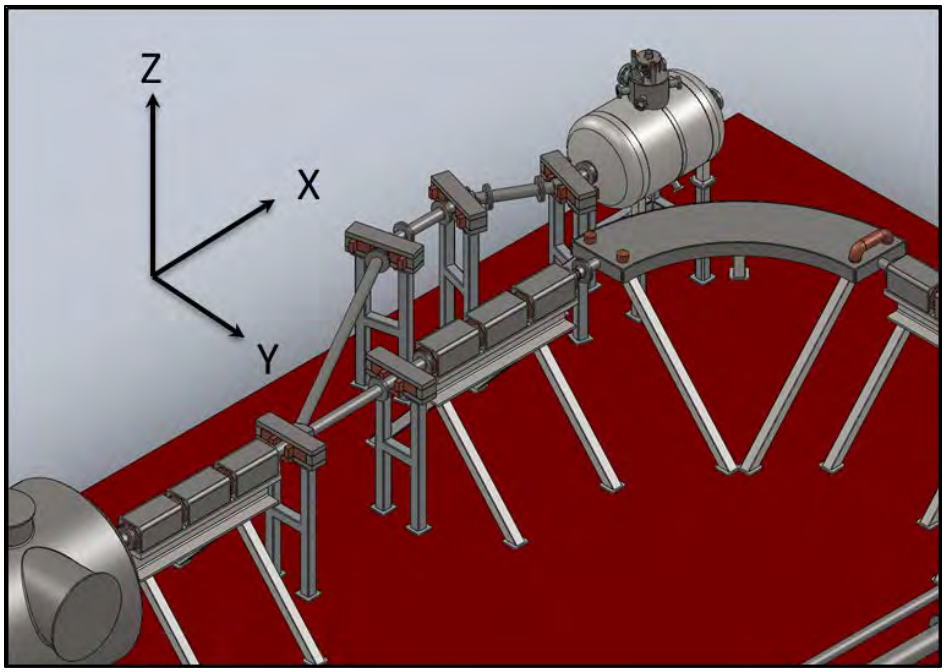

Figure 19. Injector Assembly and Merge into Beam Path. Assembly Consists of Injector Cryogenic Module, Several Dipole Magnets, and Associated Piping.

a. Wave Excitation Motion

Under steady-state excitation due to sea state six wave action the motion of the injector induces a cyclic change in the length of 30 microns in the electron pulse path to the main beam line as shown in Figure 20. After some initial transient motion a regular period of 2 seconds is observed. The relatively slow rate of deformation compared to the saturation time of an oscillator type FEL would allow uninterrupted operation. Contributions to the deformation of the injector beam path from Y and Z direction displacements were insignificant compared to X axis displacements. Motion in

the X axis is most likely driven by contributions from the mass of the injector deflecting its mountings and deformation of the baseplate.

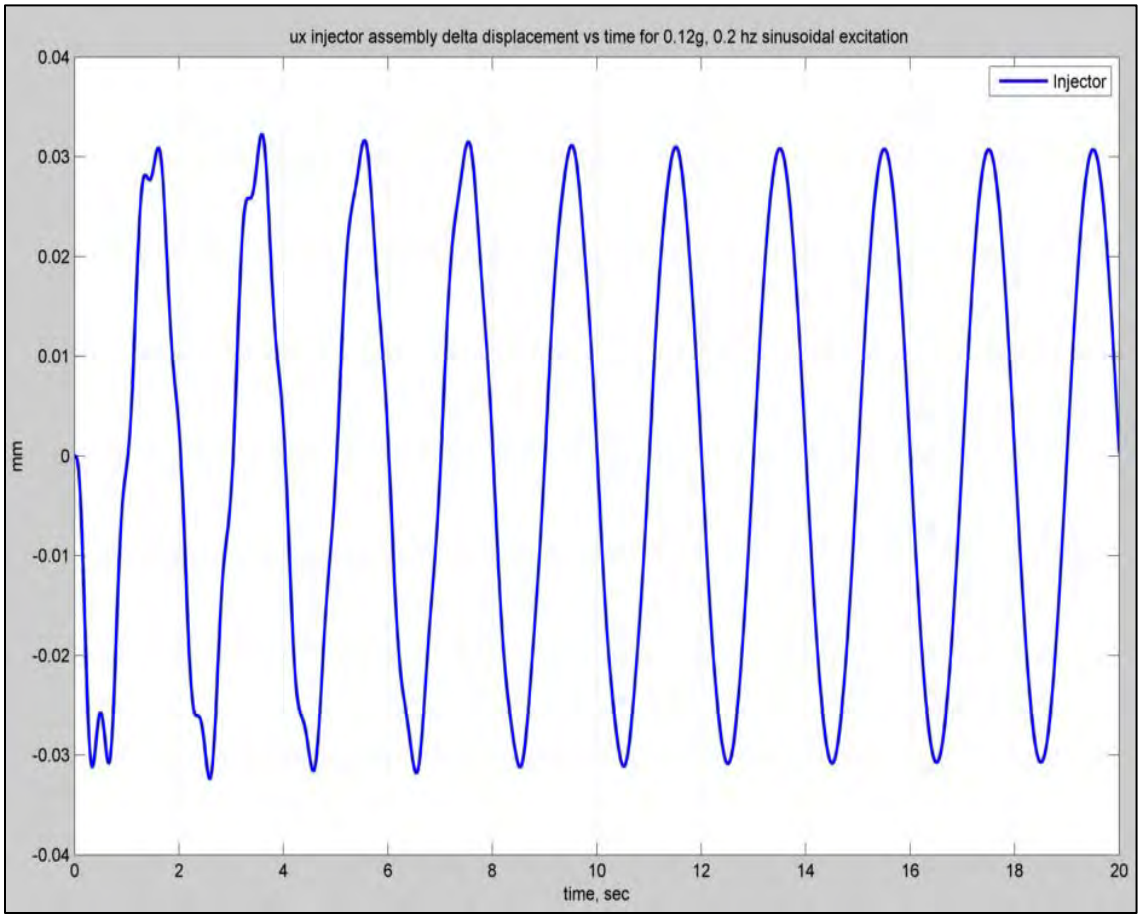

Figure 20. Wave Motion Induced Injector to Beam Path Merge Separation Distance

b. Shock Excitation Motion

When subjected to an underwater explosion, the change in length of the injector beam path reached a maximum value of 150 microns. A mild beating phenomenon can be observed in Figure 21 before damping to the steady state case over the course of 20 seconds. The one Hz isolation frequency of the isolation system is excited by the shock and evident in the resulting motion. Again the rate change of the deformation is small enough due to the long period of oscillation to allow operation.

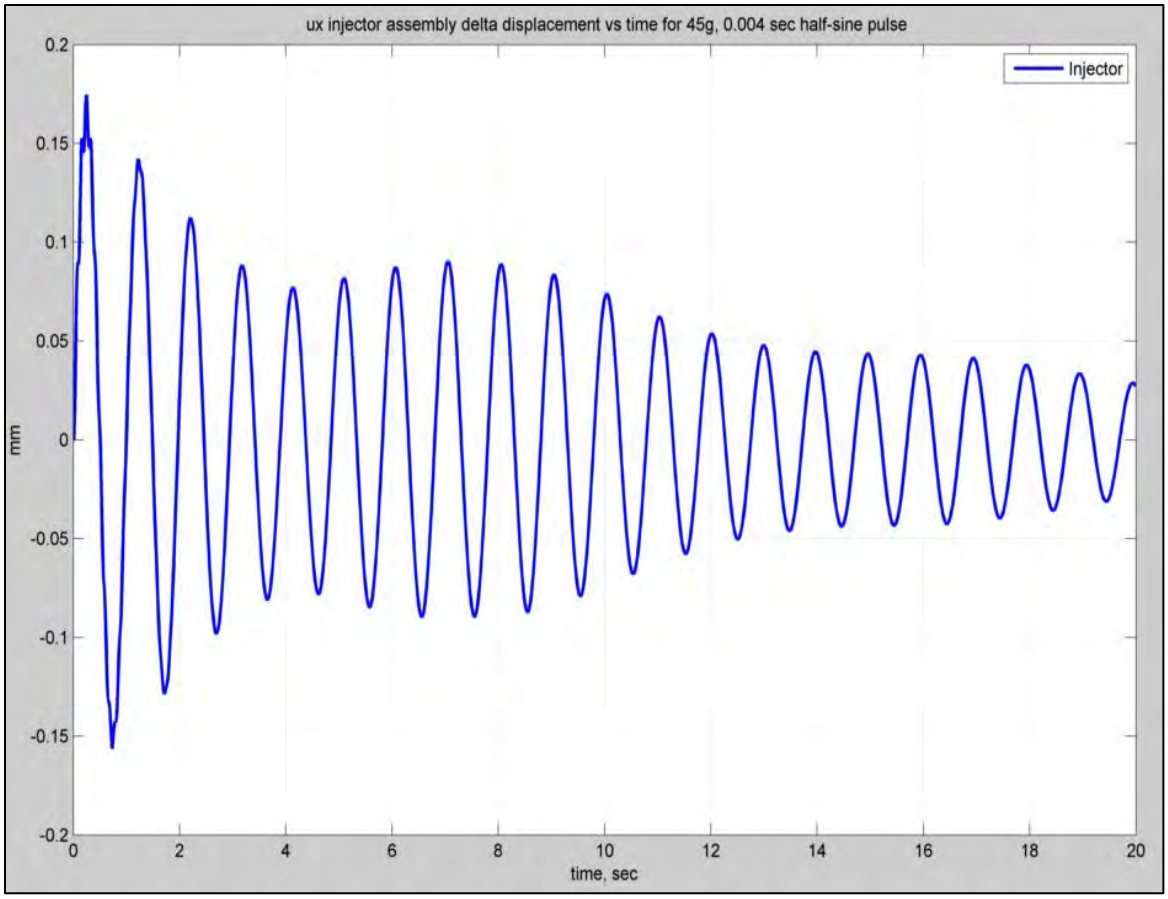

Figure 21. Underwater Explosion Induced Injector to Beam Path Merge Separation Distance

2. Undulator

The alignment and timing of the electron beam through the undulator is essential to maintaining the FEL interaction and generating laser power. The inner diameter of the evacuated beam pipe is necessarily smallest within the undulator where minimal separation of the magnets important. Figure 22 is an illustration of the undulator with inlet and outlet dipole and six alignment quadrupole magnets.

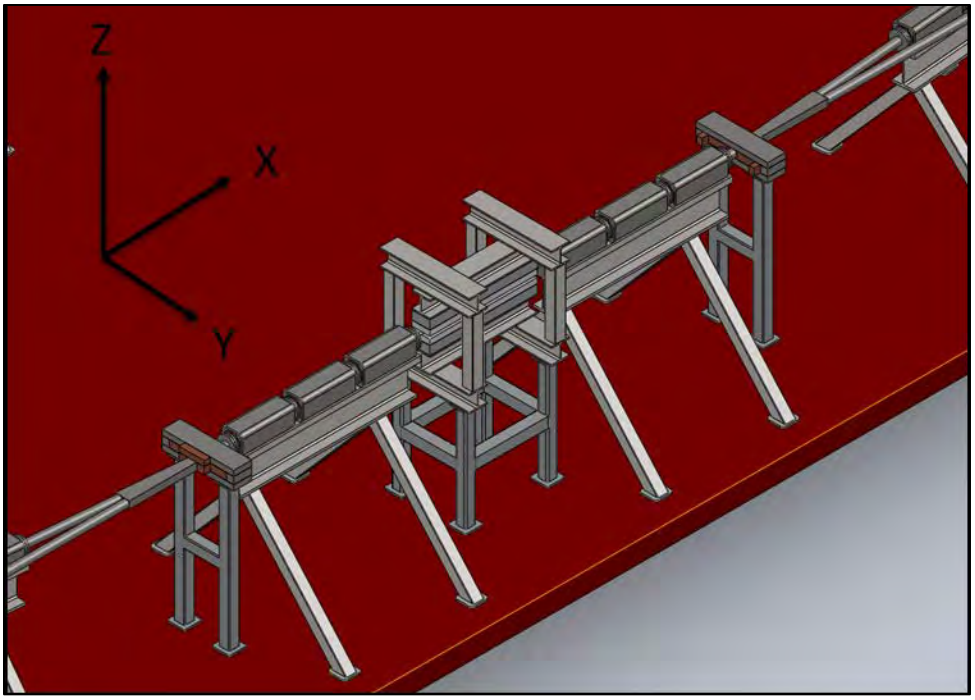

Figure 22. Undulator Assembly with Inlet and Outlet Alignment Quadrupole Magnets

a. Wave Excitation Motion

A basic concern for alignment of the undulator is assuring that the electron beam does not contact the beam pipe. Without any active controls, the alignment of components around the undulator deviated by no more than a few hundredths of a millimeter between the dipole magnets used to merge the optical and electron beam paths as shown in Figures 23 and 24. The highest frequencies observed are transients around the one Hz isolation frequency before the steady state input period of 5 seconds presents itself. The increased amplitude of the motion of the left-hand dipole is likely attributed to the influence of the motion of the beam dump. Motion in the Y direction was on the order of microns and is not shown.

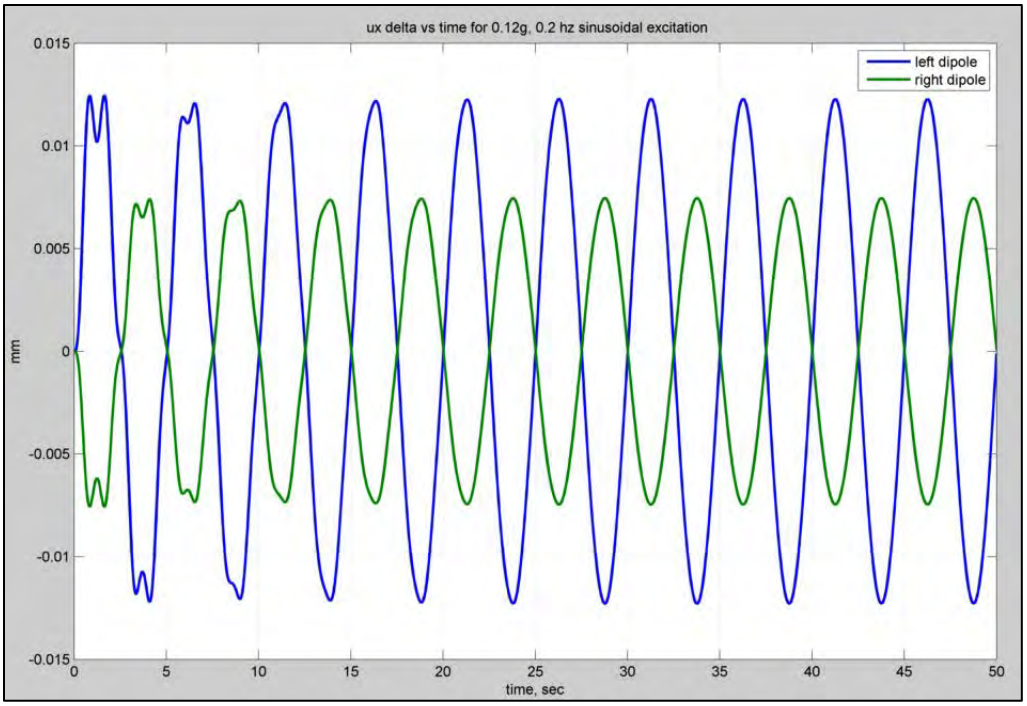

Figure 23. X Direction Steady State Undulator Inlet and Outlet Dipole Motion

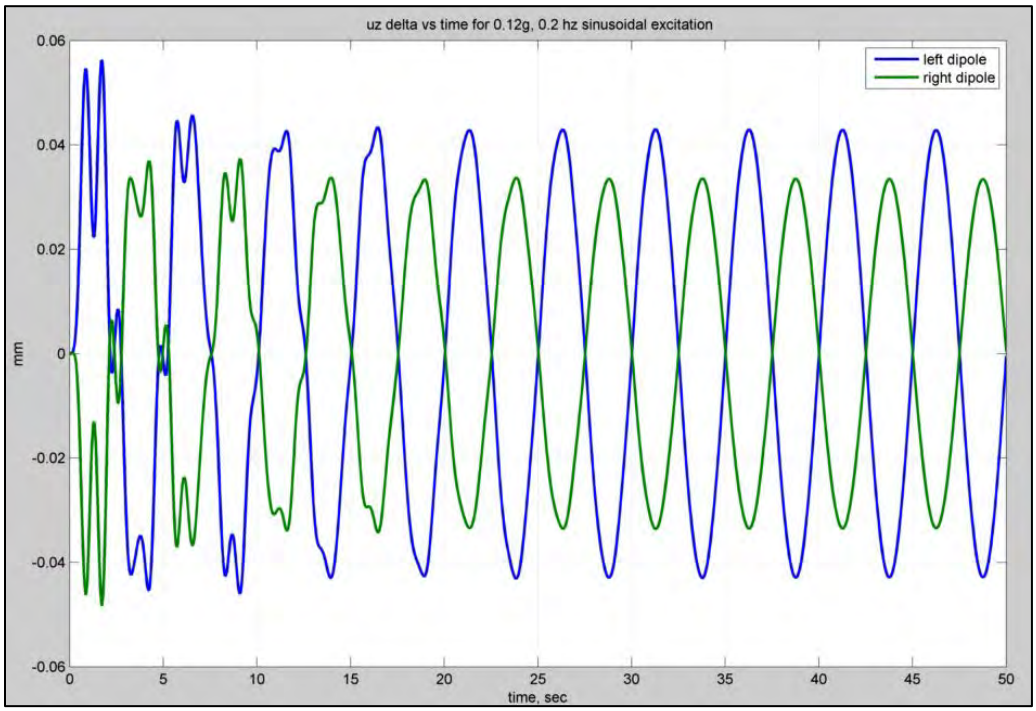

Figure 24. Z Direction Steady State Undulator Inlet and Outlet Dipole Motion

b. Shock Excitation Motion

Motion of the dipole magnets relative to the undulator due to shock trials excitation is broadly similar to the displacement seen in the steady state case. Oscillation in the X direction shows evidence of a torsional platform mode as each dipole moves out of phase relative to the undulator. Immediately after the shock was applied a maximum displacement of slightly less than one millimeter in the vertical (Z) direction occurs and subsides over the course of several beats to the steady-state case in 20 seconds as shown in Figure 26. The one Hz isolation frequency is again excited by the shock input as seen in the injector assembly. Greater amplitude of displacement is again seen occurring on the left hand side of the model and can be attributed to the large mass of the beam dump.

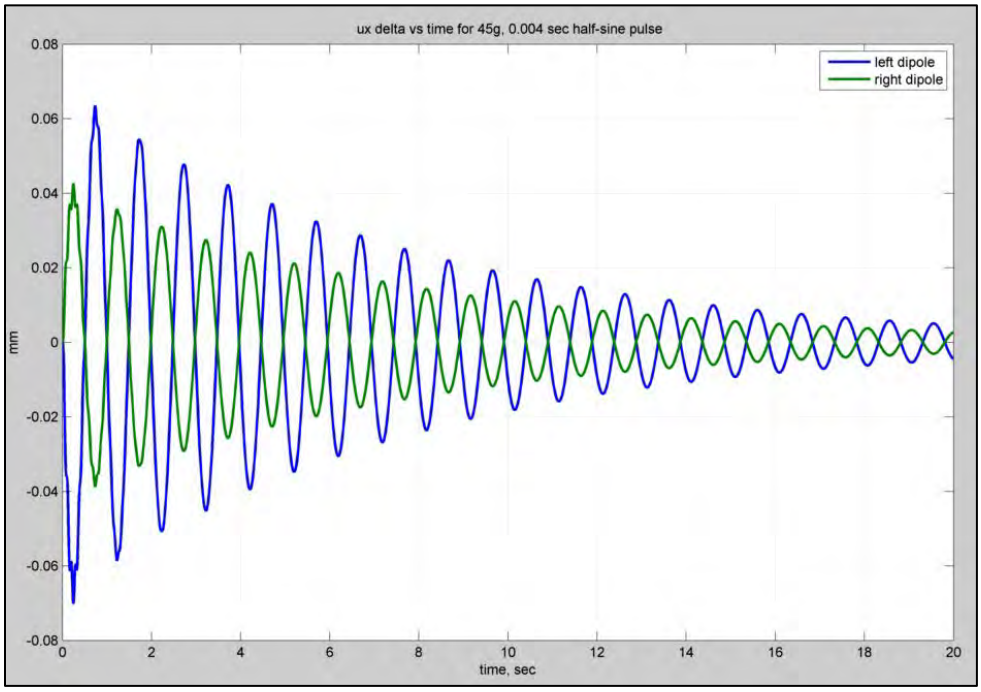

Figure 25. X Direction Shock Undulator Inlet and Outlet Dipole Motion vs. Time

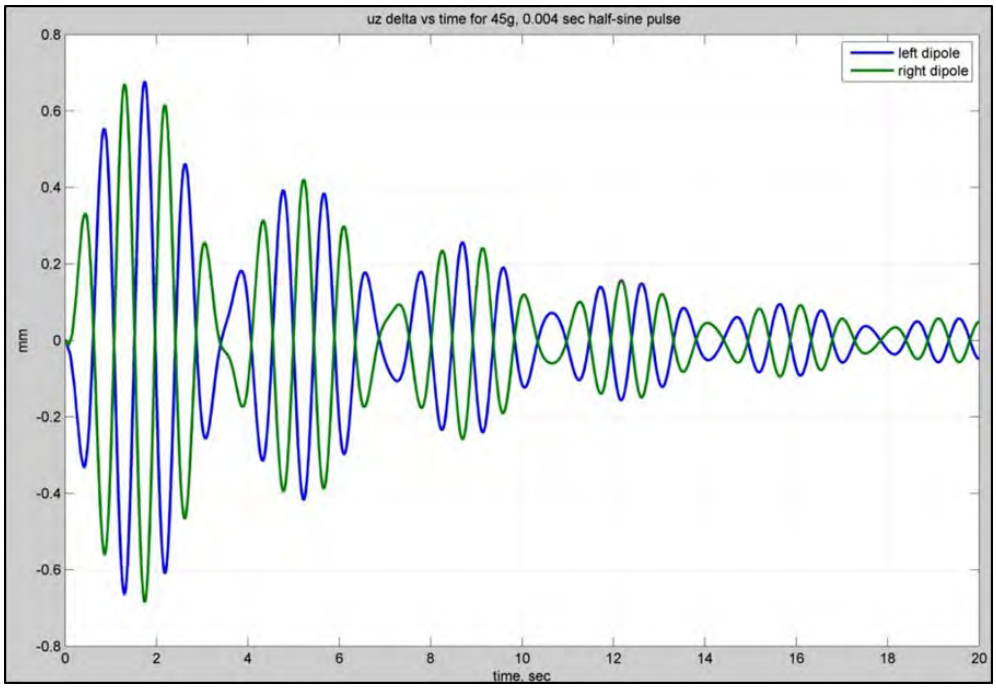

Figure 26. Z Direction Shock Undulator Inlet and Outlet Dipole Motion vs. Time

3. Beam Dump

The energy that must be removed from the beam line and the shielding required to provide adequate radiation safety are considered in the design of the beam dump. In this model, a copper core jacketed in lead is selected as a means of both dissipating heat rapidly and providing adequate shielding. The core is then surrounded by a steel water jacket through which cooling water would flow to remove the heat generated by the spent beam, as shown in Figure 27. Plumbing for the water source and sink is not included in this model and assumed to be flexible. The beam dump must maintain a reasonable alignment with the beam line, as such it is included on the isolated platform. The large mass of the beam dump once in motion influences equipment around it to a greater degree than the injector assembly, which is not as massive. The final FEL design must carefully consider the placement of the beam dump to reduce its influence on platform mounted components. It may be best to have the beam dump off the isolated platform since alignment tolerances are less severe than the injector, undulator, and most other parts of the FEL system.

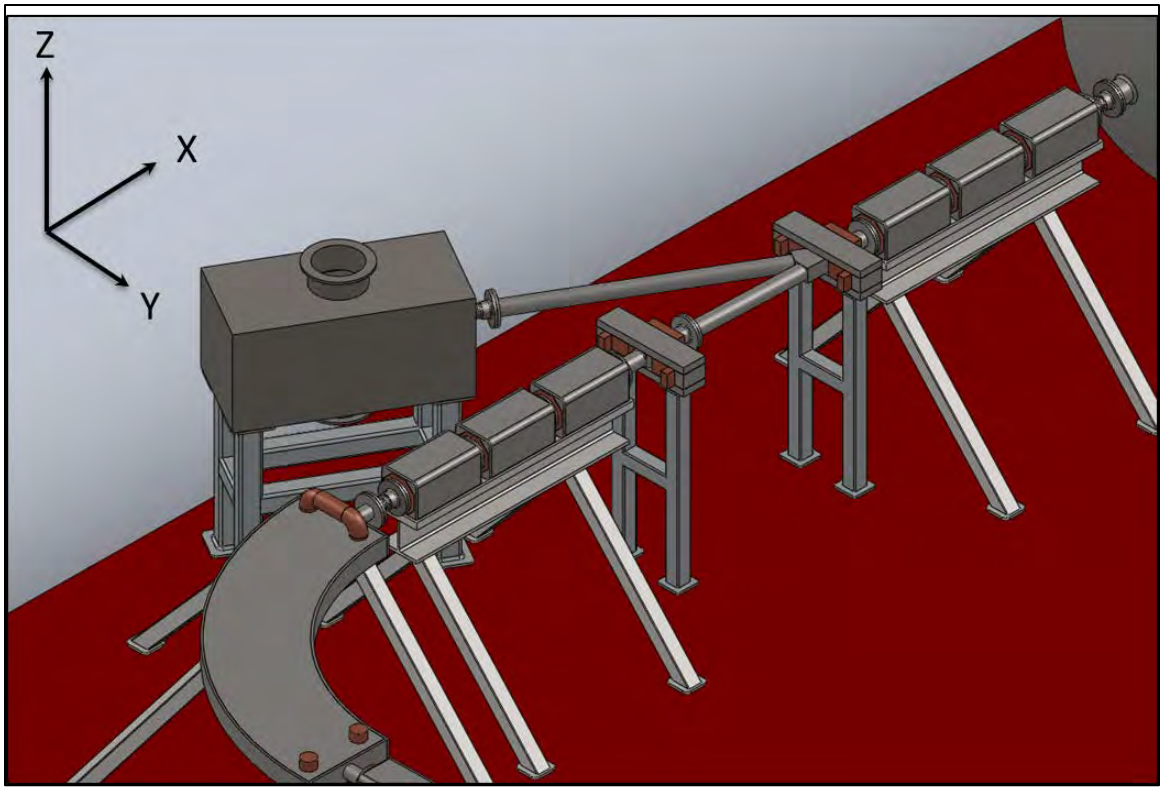

Figure 27. Beam Dump and Beam Path Split

a. Wave Excitation Motion

The steady-state motion of the beam dump due to wave excitation in the three primary axes is shown in Figures 28–30. The Y direction motion of the beam dump of one millimeter was the most significant of the three and may be a source of displacement in the beam line. Initial transient motions occur slightly above one Hz before damping to a sub-Hz steady-state motion with a period of around two seconds. The Z direction motion is shown relative to the merge with the main beam path. The inlet and rear of the beam dump move uniformly together along all the primary axes under steady-state excitation.

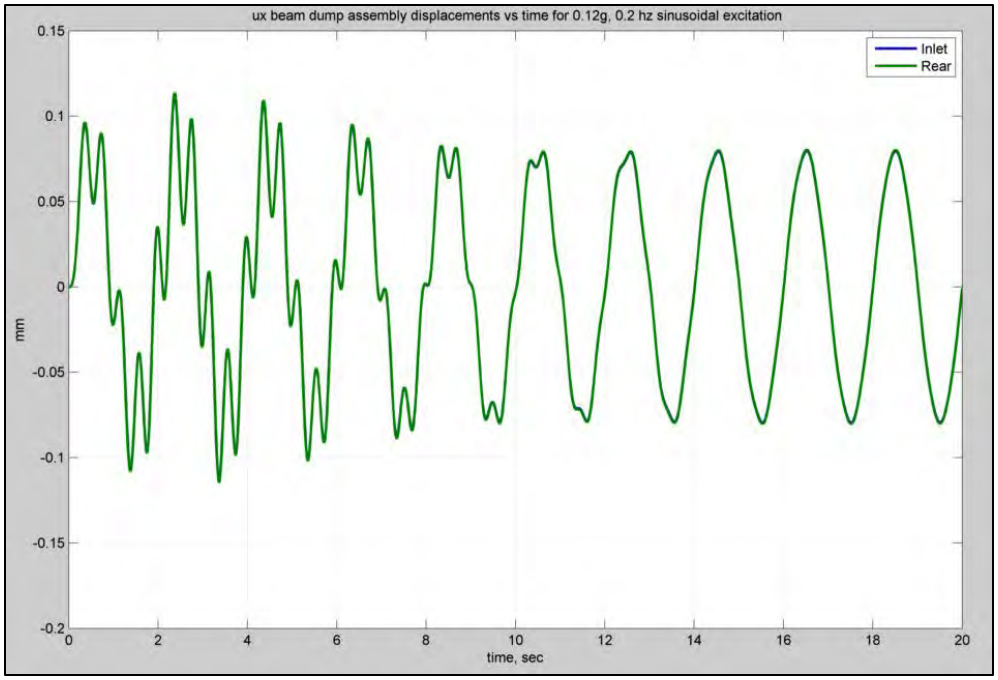

Figure 28. Steady State Beam Dump X Direction Displacement

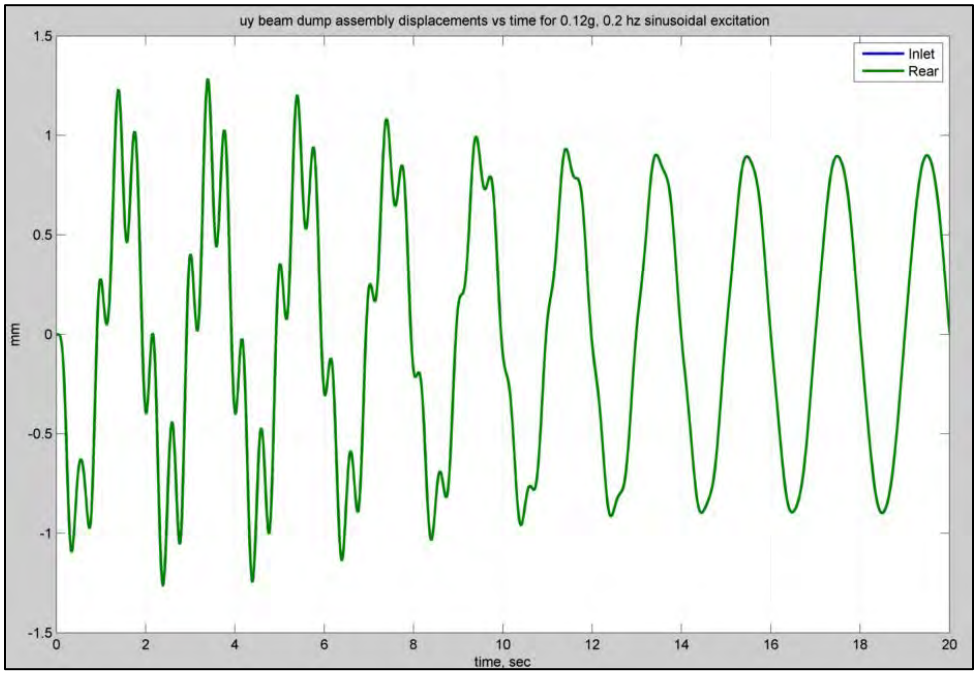

Figure 29. Steady State Beam Dump Y Direction Displacement

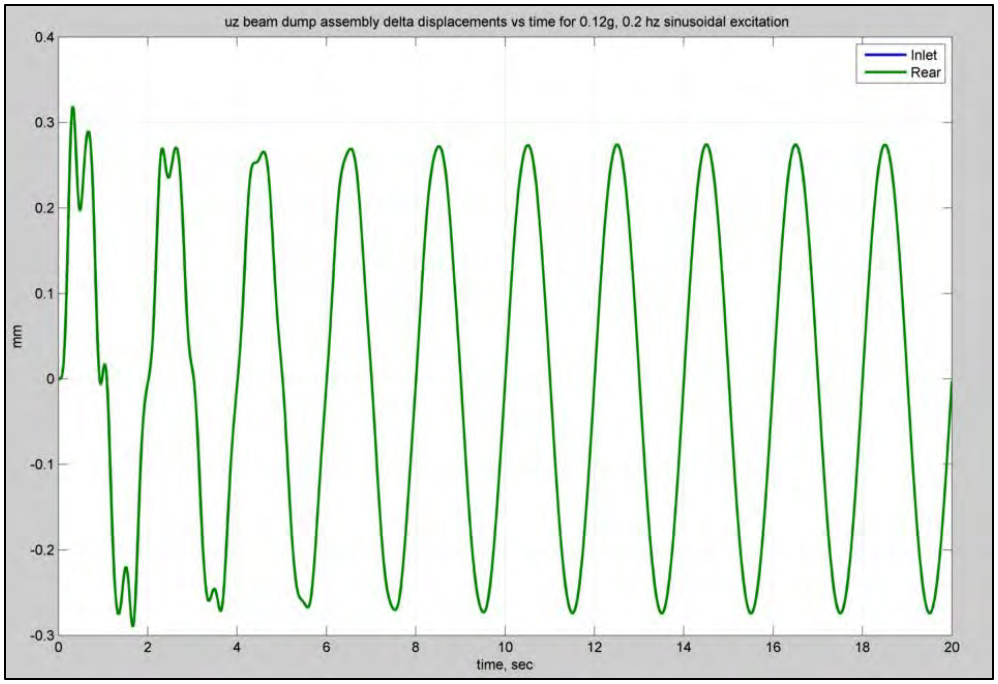

Figure 30. Steady State Beam Dump Z Direction Displacement Relative to Beam Path

b. Shock Excitation Motion

The shock motion of the beam dump due to an underwater explosion in the three primary axes is shown in Figures 31–33. The Y direction motion of the beam dump of 10 millimeters was the most significant of the three and may be a source of displacement in the beam line. The Z direction motion is shown relative to the merge with the main beam path. Under shock excitation, a significant difference in the motion of the inlet and rear of the beam dump is evident in the Z direction. Bending mode excitation of the platform along the X and Y axes is a likely explanation of this motion. In all cases the excitation of the one Hz isolation frequency under shock loading is evident.

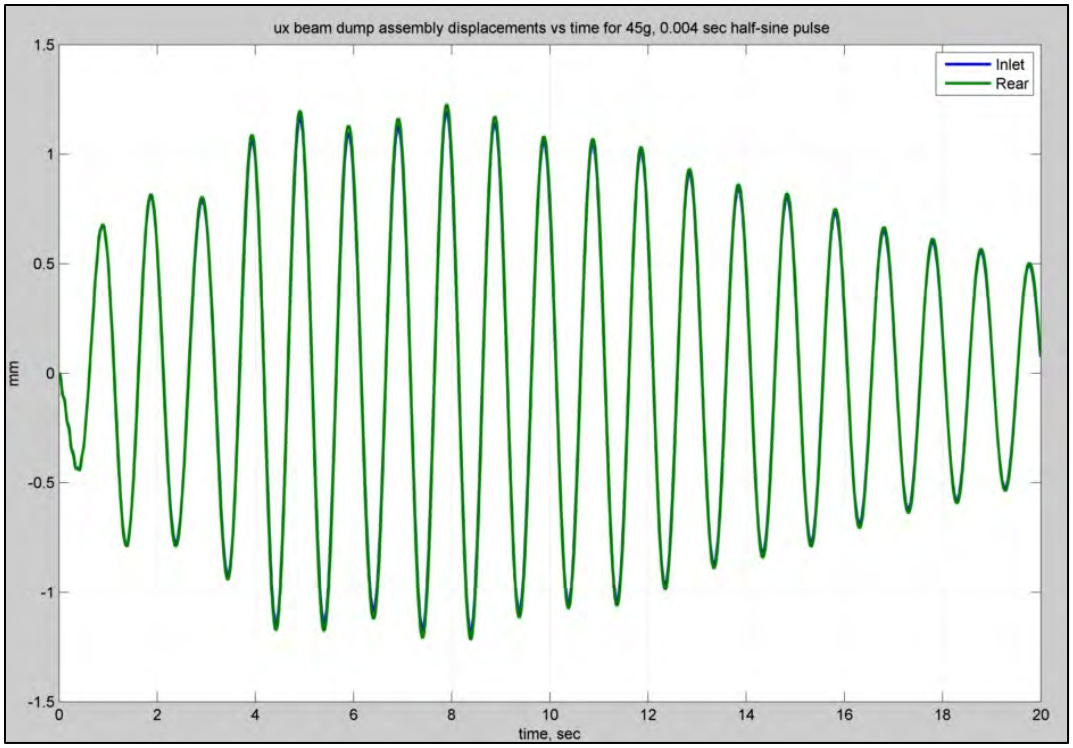

Figure 31. Shock Excitation Beam Dump X Direction Displacement

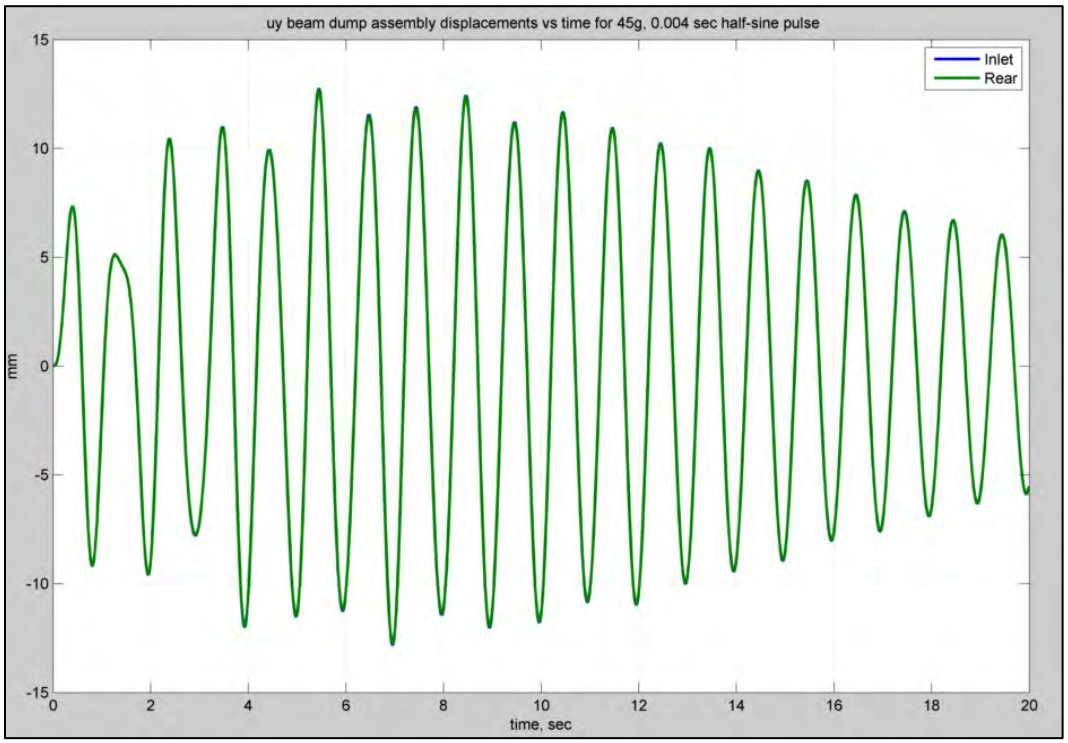

Figure 32. Shock Excitation Beam Dump Y Direction Displacement

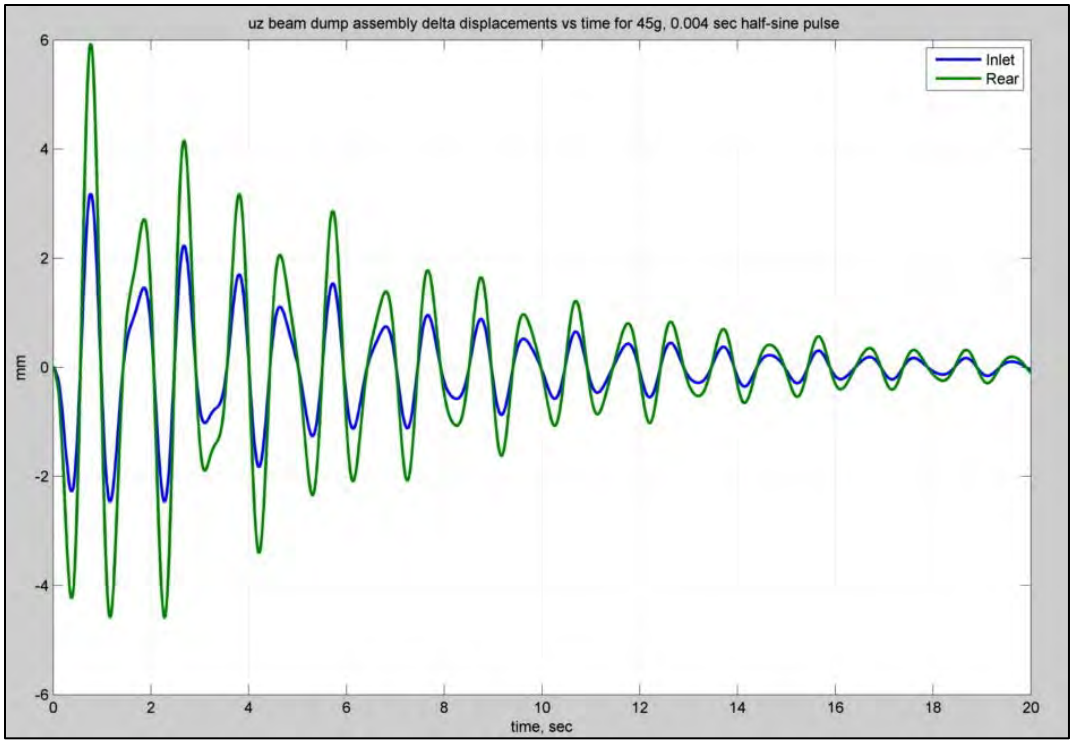

Figure 33. Shock Excitation Beam Dump Z Direction Displacement

4. Beam Path "Racetrack"

Timing between the arriving bunches of electrons and the light resonating in the optical cavity is very important. Deviation of the beam path between the LINAC module and the undulator could affect the arrival time of electrons and reduce the output laser power to zero. Figure 34 shows the "racetrack" path from the LINAC module outlet to the undulator and back to the LINAC module inlet. Timing tolerances for the return path are significantly less severe than for undulator inlet side. Within the beam path components the electron beam is actively steered with an update rate in the kHz range allowing it to compensate for component motion rapidly.

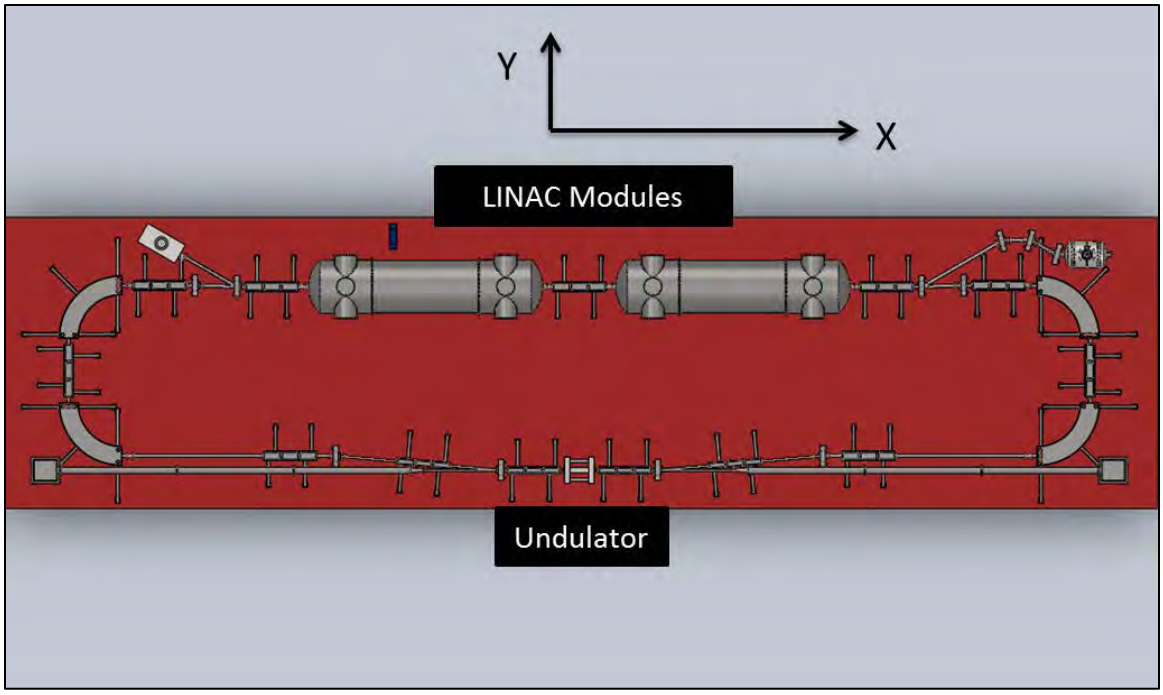

Figure 34. Top View of Beam Path "Racetrack"

a. Wave Excitation Motion

Under steady-state wave excitation, the change in length of the beam path from the outlet of the LINAC to the inlet of the undulator, and the length back to the LINAC inlet were calculated, as shown in Figures 35 and 36. Under steady-state wave excitation, the deformation of the beam line from the LINAC to the undulator was significantly greater than the return path with a nearly 4 millimeter expansion and contraction oscillating through a 2 second period after the initial transient response. The only non-symmetric components of the FEL about the Y axis are the injector and beam dump. Again it appears that the mass of the beam dump is driving deformation of the beam line. Similar to the case of the injector path distortion, the slow rate of change in the length of the beam path should allow the laser to operate. The FEL interaction of an oscillator type machine should compensate for change in the beam path length naturally as the optical resonator will follow the electron beam phase shift as long as the shift is sufficiently slow. For the case of an amplifier type FEL, the change in length of the beam path must be compensated for to ensure a proper interaction with the seed laser.

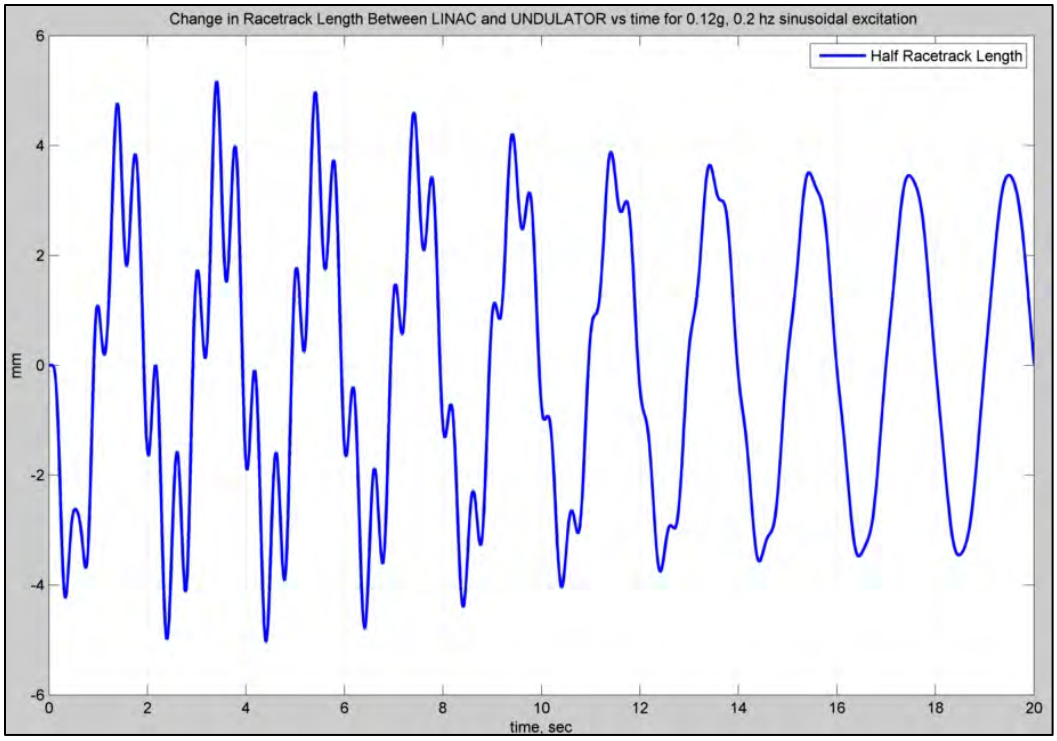

Figure 35. Steady State Change in Beam Path Length: LINAC to Undulator

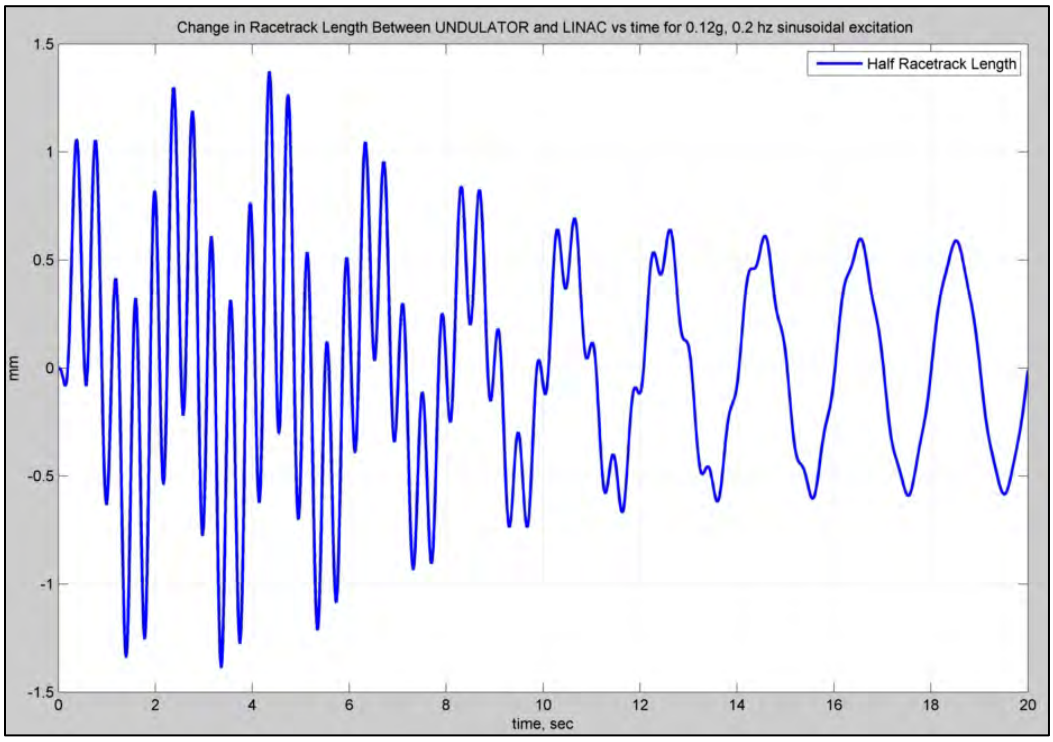

Figure 36. Steady State Change in Beam Path Length: Undulator to LINAC

b. Shock Excitation Motion

The length of the beam path from the outlet of the LINAC to the inlet of the undulator, and the length back to the LINAC inlet are calculated due to an underwater explosive shock. As with the steady-state wave excitation case, the deformation of the beam line from the LINAC to the undulator was nearly double that of the return path. Similar to other shock loaded cases, placement of heavy components, such as the beam dump, and their coupling to the beam line is of critical importance to any future FEL models. It is recommended that the beam dump be removed from the platform in future designs.

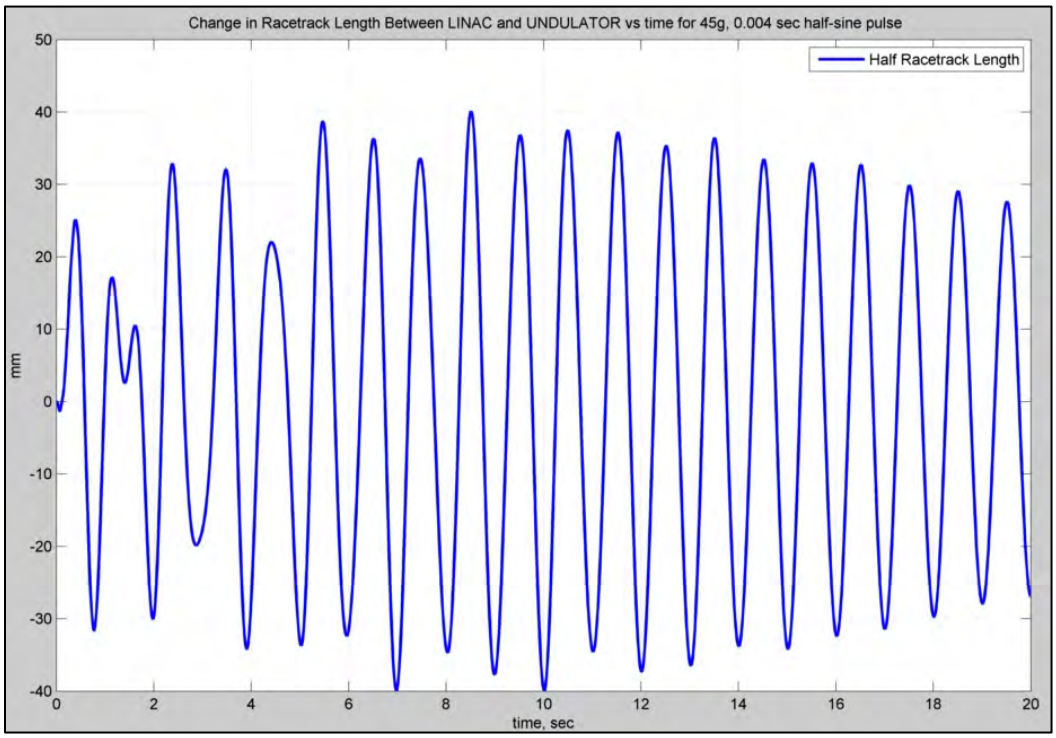

Figure 37. Shock Excitation Change in Beam Path Length: LINAC to Undulator

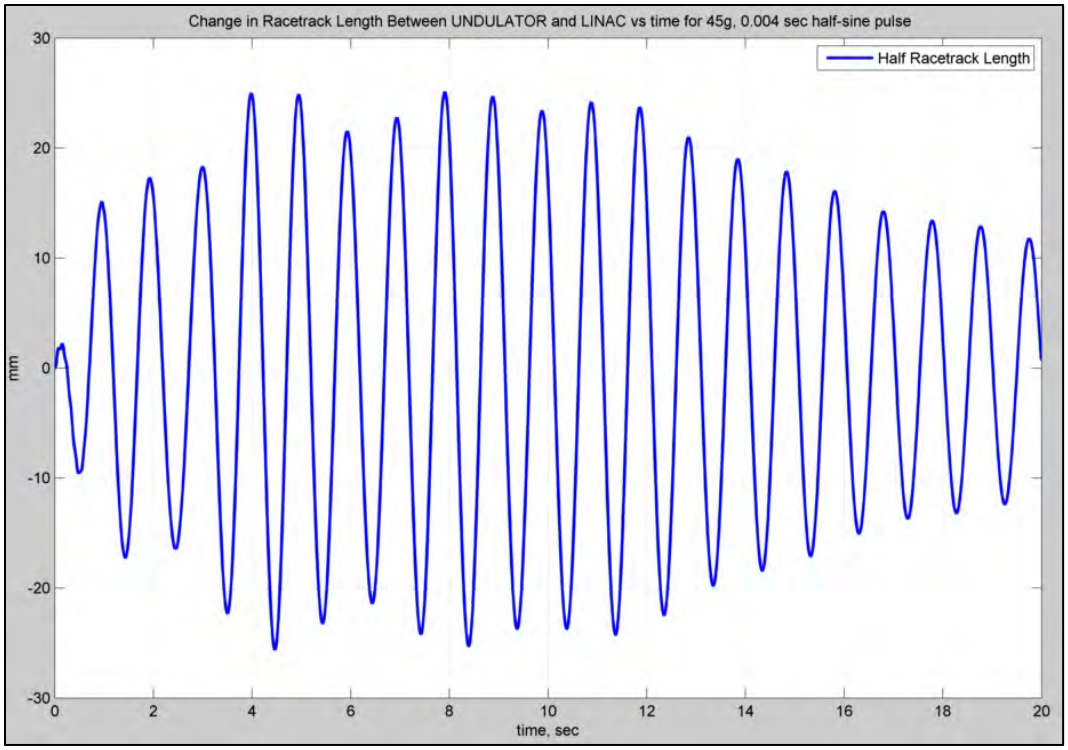

Figure 38. Shock Excitation Change in Beam Path Length: Undulator to LINAC

V. CONCLUSIONS

A. FINDINGS

1. Simulation Methodology

The complex FEL system is represented as a simple model that sufficiently characterizes the full system motion and allows simulations to be run rapidly on basic computing hardware. When more detailed and finalized shipboard FEL designs become available the same method for virtual vibration testing could easily be applied. Using a simplified model for simulation allows for rapid configuration changes and evaluation. Many of the basic principles found here can be helpful in developing a more mature design.

2. Passively Isolated Platform

The passively isolated platform provides both the stiffness required to maintain component alignment while largely decoupling the system from the motion of the hull. Selecting a platform with roughly a decade of separation between its lowest normal mode frequency and the natural frequency of the isolation system has been shown to be effective at minimizing the motion of supported FEL equipment. Separating the isolation system frequency from the frequencies of excitation sources again has been found to reduce the motion of isolated components.

3. Electron Beam Path

Investigation into the motion of electron beam line components demonstrated the need to minimize non-symmetrical mass distribution. When final shipboard FEL system models are being developed, care must be taken to place heavy components as near the centers of bending as possible to minimize deformation of the platform. Decoupling the beam line from the injector and beam dump assemblies should be a priority in any future FEL system designs. The beam dump may be removed from the isolated platform entirely.

The electron beam path will require active electron beam control systems to maintain the FEL interaction timing tolerances within the undulator; however passive controls alone appear to be enough to maintain an alignment where clearance between the beam and beam pipe is maintained.

B. FUTURE WORK

1. Active Platform Control

This model only considered passive control of the FEL mounting platform as a means of reducing the amplitudes of component motion which would be further corrected using active control mechanisms [16]. Active control of the platform in addition to the components mounted on it could again reduce the excitation transmitted to the system and the amplitude of component motion.

2. FEL System Auxiliaries Integration

This model did not consider integration and isolation of FEL auxiliary systems. When future FEL systems designs are finalized, attention must be paid to the integration of electrical power, RF energy sources, cooling water, and cryogenic equipment. Methods must be developed to prevent off platform vibrations from being transmitted to equipment via auxiliary equipment connections. Isolation of vibrating equipment that must be mounted on the platform must also be considered.

3. Flexible Hull Model

This model only considered the rigid body motion of the ship's hull. Exploring the motion of any rigidly mounted FEL equipment will require an accurate model of how a ship's hull bends under wave and underwater explosive shock excitation.

LIST OF REFERENCES

[1] W. B. Colson, "Vibration Tolerance of Free Electron Lasers.", Naval Postgraduate School. 8 August 2011.

[2] G. Neil. "Jlab FEL footprint" Personal Email (2011, Jun. 10)

[3] Military Specification, MIL-STD-167-1A, "DOD Test Method Standard: Mechanical Vibrations of Shipboard Equipment", Nov. 2005.

[4] FELSIM version 2.3. Princeton, New Jersey: Advanced Energy Systems Inc. , 2011.

[5] R. Jecks. "Niowave Contact" Personal E-mail (2011, Feb. 07)

[6] *ANSYS Command Reference*. Canonsburg, SAS IP, 2009

[7] Y. Saad, *Numerical Methods for Large Eigenvalue Problems*. London, Halsted, 1992.

[8] R. F. Beck, and A. Troesch, *Documentation and User's Manual for the Computer Program SHIPMO.BM*. Ann Arbor: n.p , 1989

[9] *Guide to Meteorological Instruments and Methods of Observation 7th ed.,* Geneva, World Maritime Organization, 2008

[10] NAVSEA 0908-LP-000-3010A, Shock Design Criteria for Surface Ships, October 1994.

[11] D.T. Hart and Y.S. Shin, "Shock Trial Simulation of USS Winston S. Churchill (DDG-81): Surrounding Fluid Effects," Dept. Mech. Eng., Naval Postgraduate School, Monterey, CA, March 2003.

[12] M. R. Hatch, *Vibration Simulation Using MATLAB and ANSYS*. Boca Raton: Chapman & Hall/CRC, 2001

[13] Firestone Industrial Products Company. *Airmount Engineering Manual and Design Guide*. Indianapolis, BFS Diversified Products, 2004.

[14] M. Evert. "Follow up for FEL optical bench" Personal E-mail (2011, Oct. 28)

[15] G. Fountain, *CSA Engineering Team Helps Stabilize Directed Energy Beam in Successful Anti-Ballistic Missile Airborne Laser Test*.[pdf]. Available: http://www.csaengineering.com/literature

[16] Rao, Singresu. Mechanical Vibrations. New York, Addison-Wesley, 1995.

[17] MATLAB version 7.11.0. Natick, Massachusetts: The Mathworks Inc., .2010.

[18] ANSYS version 13. Canonsburg, Pennsylvania. ANSYS Inc., 2010.

INITIAL DISTRIBUTION LIST

1. Defense Technical Information Center
   Ft. Belvoir, Virginia

2. Dudley Knox Library
   Naval Postgraduate School
   Monterey, California

3. William B. Colson
   Naval Postgraduate School
   Monterey, California

4. Fotis Papoulias
   Naval Postgraduate School
   Monterey, California

5. Keith R. Cohn
   Naval Postgraduate School
   Monterey, California

6. Michael R. Hatch
   Mountain View, California

7. Mike Evert
   CSA Engineering
   Mountain View, California